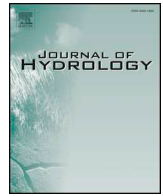




ELSEVIER

Contents lists available at ScienceDirect

Journal of Hydrology

journal homepage: www.elsevier.com/locate/jhydrol

Research papers

Characterization of vertical unsaturated flow reveals why storm runoff responses can be simulated by simple runoff-storage relationship models

Makoto Tani^{a,*}, Yuki Matsushi^b, Takahiro Sayama^b, Roy C. Sidle^c, Nagahiro Kojima^d

^a Faculty of Human Environment, University of Human Environments, 6-2 Kamisanbonmatsu, Motojukucho, Okazaki, Aichi 444-3505, Japan

^b Disaster Prevention Research Institute, Kyoto University, Gokasho, Uji, Kyoto 611-0011, Japan

^c Mountain Societies Research Institute, Earth and Environmental Sciences, University of Central Asia, Khorog GBAO 736000, Tajikistan

^d Lake Biwa Environmental Research Institute, 5-34, Yanagigasaki, Otsu, Shiga 520-0022, Japan

ARTICLE INFO

This manuscript was handled by Marco Borga, Editor-in-Chief

Keywords:

Hillslope hydrology
Storm runoff response
Vertical unsaturated flow
Soil hydraulic properties
Runoff-storage relationship

ABSTRACT

Numerical experiments on vertical unsaturated flow using the Richards equation were conducted to examine the physical basis of why storm runoff responses from mountainous watersheds in tectonically active regions could be simulated by simple runoff models with a runoff-storage power-law relationship. Pressure head propagation transmitted through vertical unsaturated flow could produce a rapid response of the outflow from bottom of the soil column, regardless of the inherent soil hydraulic properties, similar to storm runoff responses observed on a hillslope in a ‘constant allocation period’ when a large constant portion of rainfall is allocated to storm runoff. Additional experiments were conducted both for an increasing stage of downward flux in response to increasing rainfall intensity and for a recession stage without rainfall, to investigate the detailed characteristics of vertical unsaturated flow. The creation of a wetting front during the increasing stage delayed the increase of outflow, but this delay was small during a constant allocation period. An interdependent relationship between the outflow rate and the total storage of the soil column throughout the recession stage was approximated by a power-law equation derived from relationships between total storage and constant outflow under steady-state conditions. The exponent of the power-law equation approached a maximum of unity as the column length decreased, and it approached the minimum value obtained from the intrinsic relationship between soil hydraulic conductivity and volumetric water content as the column length increased. The interdependence of the outflow rate with the total storage generally detected only in the unsaturated zone might cause a low sensitivity of outflow responses to the heterogeneities of soil hydraulic properties, justifying the application of simple runoff models in heterogeneous mountain watersheds.

1. Introduction

Predicting stream runoff responses to large-magnitude storms is critically important to mitigate severe flood hazards in tectonically active regions, including Japan and other circum-Pacific regions (Tsukamoto and Minematsu, 1987; Sidle et al., 2006; Sidle and Bogaard, 2016). It was already found over a half century ago that storm runoff responses could be roughly simulated by simple runoff models (Sueishi, 1955; Nash, 1960; Sugawara, 1961), but we have not clearly understood what hydrological processes dominantly control the responses (Fatichi et al., 2016; McDonnell et al., 2007; Montgomery and Dietrich, 2002; Chiffard et al., 2019). It is difficult even now to determine what watershed characteristics each parameter of such a simple runoff model may physically reflect. Therefore, to couple studies on the runoff model development with those on storm-runoff generation

mechanisms is still a fundamental subject in hydrological sciences.

In this paper, we try to examine the physical meaning included in a model parameter by selecting the storage function model (SFM) proposed by Kimura (1961). This lumped runoff model includes a power-law relationship between storage and discharge as the core equation; this model is the standard tool for projects undertaken by the Ministry of Land, Infrastructure, Transport and Tourism (Project for the Enhancement of Capabilities in Flood Control and Sabo Engineering of the DPWH, 2002), and has been widely used throughout Asia (Sugiyama et al., 1997; Park et al., 1999; Wu et al., 2011; Gopalan et al., 2018). On the other hand, various types of runoff models emphasizing increasingly detailed hydrological processes have been proposed in the past half century (Beven, 2012), but the relatively simple application of the SFM suggests there are two kinds of general characteristics (discussed below) included in watershed hydrological

* Corresponding author.

E-mail address: m-tani@uhe-ac.jp (M. Tani).

<https://doi.org/10.1016/j.jhydrol.2020.124982>

processes regardless of its simple and rather old-fashioned structure.

One characteristic provided by the SFM is derived from the concept of 'saturated rainfall'. The SFM assumes the area contributing to a storm runoff response is limited to a portion of the watershed at the beginning of a storm event, but that the contributing area is spatially extended by a sequence of rainfall. Kimura (1975) defined saturated rainfall as the cumulative rainfall at the time when the contribution area reaches the entire watershed and considered that the ratio of rainfall allocated to the storm runoff had a constant value, called as the saturated runoff ratio (Park et al., 1999). This concept has been accepted in many studies on runoff analysis; a recent study by Supraba and Yamada (2015) investigated storm runoff responses in 36 mountainous watersheds in Japan and demonstrated that all the rainfall was allocated to storm runoff after the cumulative rainfall reached the saturated rainfall in 23 watersheds, the value of which ranged from 81.8 mm to 170.9 mm. The saturated runoff ratio may be regarded as unity for these watersheds.

However, this result should be checked because the simple concept of saturated rainfall in the SFM was empirically obtained from runoff analysis to simulate runoff responses to storms at a watershed scale and did not specify detailed hydrological mechanisms at a hillslope scale (Kimura, 1975). First, we have to consider that the value of runoff ratio for storm runoff responses may be affected by the underestimation of watershed-mean rainfall particularly in mountainous regions (Tani, 1996; Arnaud et al., 2011). Even though the rainfall records are sufficiently accurate, the runoff ratio should be lower than unity; this is caused both by forest-canopy interception during a storm event (Murakami, 2006) and leakage into the deep underground structure where groundwater does not contribute to storm runoff response (Katsuyama et al., 2008).

From this perspective, we refer to a sprinkler experiment conducted in watershed CB1 in Oregon Coast Range, USA (Montgomery et al., 1997; Anderson et al., 1997; Torres et al., 1998). Sprinkled water was supplied at constant intensity onto a small unchanneled watershed for several days, and runoff reached a constant rate although the rate per unit watershed area was lower than the rainfall intensity due to losses including evapotranspiration and infiltration into the underlying bedrock. However, the actual input rate of the sprinkled water had a diurnal oscillation due to an influence of evapotranspiration and this was reflected by a gentler diurnal oscillation in the output runoff rate, and the period with constant runoff rate was called as 'quasi-steady state' (Montgomery et al., 1997). This result suggested that such a period is important for analyzing runoff generation mechanisms even if the runoff ratio is less than unity and the input rainfall is not with a constant intensity. Certainly, the concept of saturated rainfall was only empirically obtained from runoff analyses by the SFM, but the period, when the rainfall exceeds the saturated rainfall, may contribute to an elucidation of complex storm runoff mechanisms because we can assume the stormflow contribution area does not change anymore. Hence, we define 'constant allocation period (CAP)' as the period when a large constant portion of rainfall is allocated to storm runoff. Our analysis in this paper focuses on stormflow generation processes only in CAP to avoid the complexity derived from the temporal and spatial variability of stormflow contributing area (Hewlett and Hibbert, 1967).

The second characteristic of SFM assumes that the functional relationship between the runoff rate and storage is a simple power-law equation, which can be described with the continuum equation as:

$$S_f = kq_f^p \quad (1)$$

$$\frac{dS_f}{dt} = r - q_f \quad (2)$$

where S_f and q_f are the watershed storage (L) and the runoff rate (L T⁻¹) per unit watershed area calculated by SFM, r is the rainfall intensity (L T⁻¹), and p (dimensionless) and k (L^{1-p} T^p) are empirical parameters. Eqs. (1) and (2) imply that runoff rate can be obtained from watershed storage by a one-to-one relationship, and the equation set

composed of Eqs. (1) and (2) included in SFM is hereinafter referred to as SFE in this paper. Hysteresis between storage and runoff has been already recognized since the original proposal of SFM (Kimura, 1975), and the one-to-one relationship can only be an approximation. Nevertheless, the SFE has been included as a component in many runoff models including the Tank model (Sugawara, 1961, 1995), HBV model (Bergström and Forsman, 1973), HCYMODEL (Fukushima and Suzuki, 1988; Tani et al., 2012), and the NAM model (Madsen, 2000). Therefore, a major question in hillslope hydrology is why a simple equation set like SFE provides adequate descriptions of runoff responses despite the litany of stormflow generation mechanisms identified by previous studies.

These two characteristics of SFM may suggest that a CAP is created in response to a large magnitude storm, where cumulative rainfall exceeds saturated rainfall, and that the temporal change in runoff (hydrograph) produced from the rainfall (hyetograph) may be approximated by SFE. Considering only the CAP, we can focus on analyzing the simple conversion process from the hyetograph to the hydrograph within the fixed runoff contribution area. Our paper aims to elucidate the hydraulic mechanism at the hillslope scale that produces storm-runoff responses approximated by SFE.

Because rainfall at the ground surface is a parallel vertical flux of water moving under the influence of gravity, the first process of water movement on a hillslope may usually occur as a vertical infiltration, although the flow direction is somewhat modified by heterogeneous soil physical properties (Noguchi et al., 1999; Sidle et al., 2000; Retter et al., 2006). Of course, above-ground and soil-surface heterogeneities may disturb the parallelism: for example, the throughfall and stem flow in forest may generate a bypass flow within a preferential path (Nanko et al., 2010; Liang et al., 2011). Similarly, ground surfaces with a low permeability may promote the generation of infiltration-excess overland flow (Miyata et al., 2009). Such quick flows may contribute to the stormflow generation even if the soil matrix remains dry (Liang et al., 2009; Dusek et al., 2012). In a CAP, when most of the rainwater contributes to storm runoff responses, however, it is unrealistic to assume that all the storm runoff volume is produced only by preferential and/or overland flows. Important contributions of the soil matrix to storm runoff responses have been suggested also from many field studies showing that a large portion of the stream water during a storm event is occupied by the pre-event water (Pearce et al., 1986; Gomi et al., 2010; Iwasaki et al., 2015). Consequently, we estimate that rainwater first infiltrates vertically into the soil, and then lateral flow is generated at some depth due to decreasing permeability with depth (Beven, 1984). Each contribution of the vertical or lateral flow components may be controlled by various hillslope properties (Buttle and McDonald, 2002; Ebel et al., 2007; Mirus and Loague, 2013), and it is important to separately quantify the effects of each component on the storm runoff responses.

In a CAP, vertical and lateral flows both in the soil-matrix and preferential paths actively contribute to the storm runoff response as schematically illustrated in Fig. 1 because a large constant portion of the rainfall is allocated to the storm runoff. Among these flow components, this paper mainly focuses on elucidating the contribution of vertical flow component in the soil matrix to storm runoff responses through numerical experiments using the Richards equation. Naturally, the contribution of preferential flow should be also evaluated, and the vertical flow should be coupled with lateral flow, in order to completely understand stormflow generation mechanism on a hillslope. However, it is important to initially specify the role of vertical unsaturated flow (VUF) first because it has not been adequately understood (Tani, 1985a; Dusek et al., 2012). We will make some discussion in Sections 4.2 and 4.3 on effects of heterogeneities with preferential paths and inter-relationship between vertical and lateral flow systems.

Before we investigate the role of VUF in storm runoff responses, we have to examine whether the application of SFE to runoff responses in CAPs at a watershed scale can be applied also at a hillslope scale. This

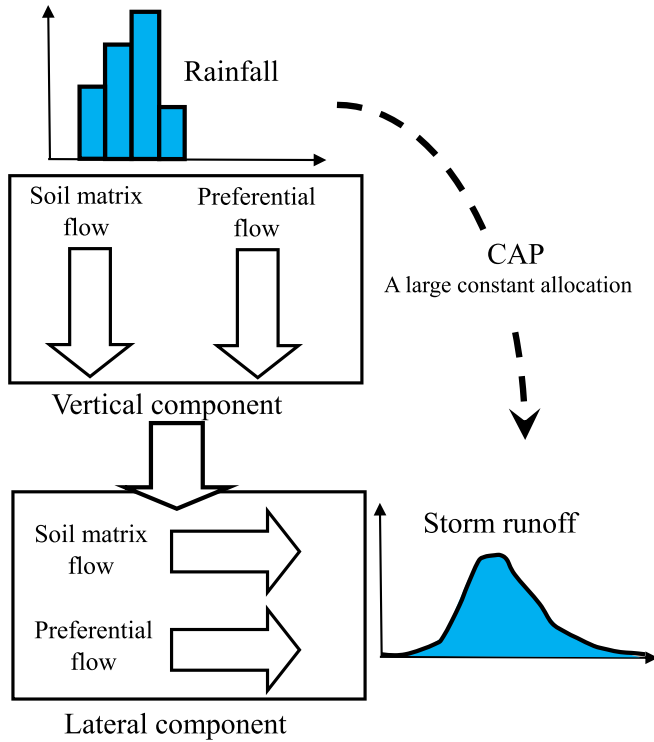


Fig. 1. Schematic diagram for hillslope flow processes contributing to storm runoff responses in a CAP.

assessment is important because scale issues derived from spatial differences from hillslopes to watersheds have been widely discussed in hydrology (Blöschl and Sivapalan, 1995; Sivapalan, 2003; McGuire et al., 2005; Clark et al., 2009; Asano et al., 2009; Sidle et al., 2017). Hence, we reanalyzed a hydrometric observation on a steep planar hillslope with a thin soil layer in Appendix 1 before we begin our main investigation using the numerical experiments by the Richards equation. Parameter values of p and k in Eq. (1) obtained from the application of SFE to the hillslope observational result will be used as a criterion to determine whether the VUF can produce storm runoff responses.

2. Method of numerical experiments

2.1. Fundamental equation

The vertical unsaturated flow (VUF) occurs as the first stage of stormflow generation on forested hillslopes as long as the soil layer is not fully saturated. We conducted numerical experiments using the one-dimensional vertical form of Richards equation for VUF in the soil column:

$$C \frac{\partial \psi}{\partial t} = \frac{\partial}{\partial z} \left\{ K \left(\frac{\partial \psi}{\partial z} + 1 \right) \right\} \quad (3)$$

where K is the hydraulic conductivity ($L T^{-1}$), C is the specific water capacity defined as $d\theta/d\psi$ (L^{-1}), ψ is the pressure head (L), θ is the volumetric water content (dimensionless), and t is time (T). The origin is placed at the bottom of the soil column, and the vertical z -axis is positive in the upward direction.

The boundary conditions at the column surface is set as:

$$f = -r \quad (4)$$

where r is the rainfall intensity ($L T^{-1}$), and f is the vertical water flux ($L T^{-1}$) defined by Darcy's law as:

$$f = -K \left(\frac{\partial \psi}{\partial z} + 1 \right) \quad (5)$$

The boundary condition at the column bottom is set to a seepage face, in which the outflow rate is calculated by a pressure head of zero at a saturated bottom condition with the rate remaining at zero for negative pressure head conditions. Because we focus our analysis on VUF only during CAP, ψ at the column bottom is always zero, indicating that the groundwater table is fixed to the bottom. This assumption might be unrealistic for a rising groundwater table, but issues on the interactions between saturated and unsaturated zones are discussed in Section 4.3.

A versatile software, HYDRUS 1D (Šimůnek et al., 2013), was adopted to get numerical solutions of the Richards equation. A physically-based Kosugi (1996) model was selected to define soil hydraulic properties because this model is derived from pore-size distribution and suitable for our purpose of parameter identification for forest soils with abundant macropores:

$$\theta \equiv (\theta_s - \theta_r) S_e + \theta_r = (\theta_s - \theta_r) Q \left[\frac{\ln(\psi/\psi_m)}{\sigma} \right] + \theta_r \quad (6)$$

$$K = K_s \left[Q \left\{ \frac{\ln(\psi/\psi_m)}{\sigma} \right\} \right]^{1/2} \times \left[Q \left\{ \frac{\ln(\psi/\psi_m)}{\sigma} + \sigma \right\} \right]^2 \quad (7)$$

where θ_s and θ_r are the saturated and residual water contents (dimensionless), S_e is the effective saturation ($L^3 L^{-3}$), ψ_m is the pressure head calculated from the median pore radius, σ is the standard deviation of the log-normal distribution of soil pore radius (dimensionless), and Q is the complimentary normal distribution function.

Note that our solutions of Eq. (3) are the temporal changes in spatial distributions of hydraulic variables (ψ , θ , and K) and flux in the vertical soil column, and that the outflow rate from the bottom can be calculated from the solutions. The runoff rate from the downslope end of the soil layer cannot be estimated from our numerical experiments because the hydraulic formula for lateral flow is not given. Regarding this limitation of ignoring lateral flow, it should be emphasized that hydraulic characteristics of lateral flow system including preferential flow paths have yet to be quantified because of their heterogeneous distributions in the soil layer even though the observational findings generally showed their important roles in quick drainage of the groundwater (Anderson et al., 1997; Sidle et al., 2000; Uchida et al., 2003) (see the discussion in Section 4.3). Hence, it may be important as an initial step for our comprehensive understanding of hillslope runoff responses to identify hydraulic behaviour in the unsaturated zone because outflow from this zone promotes subsequent lateral flow.

2.2. Soil hydraulic properties

To examine the physical basis why storm runoff responses can be widely simulated by the SFE in CAPs, it is desirable to compare the results of VUF calculated from the Richards equation using many types of soil hydraulic properties and various heterogeneous structures composed of the plural soil types. In this paper, we addressed this examination by selecting small numbers of different soil types to save a lot of energy for the comparison. For this purpose, we used five soils with homogeneous hydraulic properties: two soil types (SA and SB) were derived from the soil layer on a study hillslope (SL: 0.05 ha) (see Appendix 1). One typical forest soil (CR), one loamy soil (LM), and one soil substituted for preferential flow network (PF) were also used for our analysis. In addition, we discussed dependences of the VUF on three different stratified soil structures. The parameters of soil hydraulic properties used for our numerical experiments are listed in Table 1. The relationships of θ and K to ψ are plotted in Fig. 2(a) and (b), respectively, where the axis of ψ is given in a logarithmic scale because the relationships near the saturation should be emphasized when analyzing the behaviour in CAPs with relatively wet soil conditions.

Table 1
Soil hydraulic properties used for the numerical experiments.

(a) SA, SB, CR, LM, and PF _{Kos} by Kosugi Model.					
Soil	θ_r	θ_s	ψ_m (cm)	σ	K_s (10^{-3}cms^{-1})
SA	0.20	0.42	-10	1.7	5.0
SB	0.23	0.37	-20	1.6	5.0
CR	0.32	0.62	-25	1.6	30.0
LM	0.18	0.48	-180	1.1	0.5
PF _{Kos}	0.01	0.60	-25	0.7	58.0
(b) PF by van Genuchten model.					
Soil	θ_r	θ_s	α (cm^{-1})	n	(10^{-3}cms^{-1})
PF	0.01	0.60	0.05	3.0	58.0
(c) Soils consisting of KES by Kosugi model.					
Depth(cm)	θ_r	θ_s	ψ_m	σ	K_s (10^{-3}cms^{-1})
0-10	0.060	0.217	-157.243	2.923	82.20
10-20	0.159	0.344	-39.373	2.621	122.00
20-30	0.242	0.373	-15.209	1.722	28.80
30-40	0.239	0.323	-20.561	1.559	15.10
40-50	0.224	0.274	-29.882	1.712	11.00
50-60	0.139	0.202	-68.674	1.936	10.40
60-70	0.150	0.182	-17.785	1.087	6.18

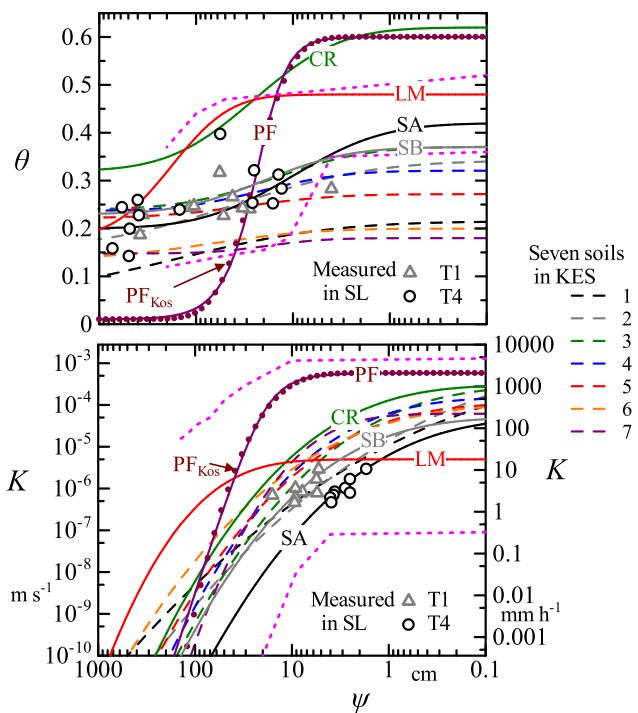


Fig. 2. Soil hydraulic properties used for the numerical experiments. (a): Relationship of volumetric water content, θ , to pressure head, ψ . (b): Relationship of hydraulic conductivity, K , to ψ . Parameter values are listed in Table 1. The range indicated by the pink dotted lines shows the parameter spaces used for the concept-development simulations by Mirus and Loague (2013).

Two soils, SA and SB, were estimated by Tani (1997) for soils at 10 cm depths the plots of which were 11.0 m (called T4) and 1.2 m (called T1) upslope from the hillslope bottom of SL with the length of 42.7 m. Because the thin soil layer at SL was not clearly stratified, we tried to simulate the pressure head values observed at 10, 30, and 50 cm depths at T4 by combining these two soils as described in Section 3.1. CR was one of the average crumb structure soils selected from a

catalogue for forest soil in Japan using the 282 samples (Mashimo, 1960), and LM was one of the average loamy soil taken from Mualem's (1976) catalogue. Parameters of soil hydraulic properties in Eqs. (6) and (7) for CR and LM were determined based on a characterization study on forest soil by Kosugi (1997a, 1997b) (Table 1a).

One additional soil PF was chosen to examine effects of preferential path network on VUF using the Richards equation, based on a dual-continuum model (Gerke and van Genuchten, 1993) developed to assess infiltration processes in vertical columns consisting of soil matrix and preferential flow domains. In this model, the preferential path network was substituted for one type of soil filled with relatively coarse particles eroded from the matrix (Vogel et al., 2010), and the soil hydraulic properties given for such a soil by Dusek et al. (2012) was also selected for PF. The values of parameters α (L^{-1}) and n (dimensionless) in the following van Genuchten (1980) model are listed in Table 1b.

$$\theta = \theta_r + (\theta_s - \theta_r)[1 + (-\alpha\psi)^n]^{-(1-\frac{1}{n})} \tag{8}$$

$$K = K_s S_e^{0.5} \left[1 - \left(1 - S_e^{\frac{n}{n-1}} \right)^{1-\frac{1}{n}} \right]^2 \tag{9}$$

The hydraulic properties for PF can be well fitted also by Kosugi model as PF_{Kos} (Fig. 2), the parameter of which are listed in Table 1a. The value of ψ_m for PF_{Kos} will be used for a discussion in Section 3.5.

We should note that because PF represents only one type of preferential paths with a small amount of fine particles, flow in other types, including pipe-like preferential paths, may give different effects on the VUF. General effects of heterogeneities including preferential paths on the VUF is discussed in Section 4.2.

We also selected three types of stratified soil structures to consider the effects of heterogeneous soil structure on VUF. One was LSA consisting of LM at depths of 0-20 cm and 50-70 cm, with SA between these layers. Another stratified structure (KES) was composed of seven layers, each with a depth of 10 cm. The properties of KES were measured in a forested hillslope at Kamigamo Experimental Station in Kyoto, Japan (Liang et al., 2009; Table 1c), and hydraulic properties of KES are inserted into Fig. 2. The third soil structure, SAB, was a combination of SA for the depth of 0-12 cm and SB for the depth of 12-70 cm.

The ranges of parameter space considered by Mirus and Loague (2013) in an investigation of runoff generation mechanisms are identified in Fig. 2 to secure the generality of our numerical experiments. The ψ - K relationships in Fig. 2b correspond approximately with the range by Mirus and Loague (Fig. 2b), but ψ - θ relationships for CR, PF, and soils included in KES extend beyond the range near saturation (Fig. 2a). However, note that differences between θ_s and θ_r for CR and soils in KES are similar to our other soil types and may control the behaviour of VUF through the value of C ($= d\theta/d\psi$) in our fundamental Eq. (3). Hence, the absolute values of θ_s and θ_r are not important to the simulation results. A large value of 0.59 in the difference of θ_s and θ_r for PF can be regarded reasonable because of the existence of preferential flow paths. Thus, we can conclude our experiments can generally describe the basic behaviour of VUF in CAP although the numbers of soil types tested are limited.

2.3. Design of experiments

Six types of numerical experiments were designed for this study. First, we conducted a comparison of results calculated through VUF with those observed in the SL (Exp. 1). The next two types of experiments aimed to determine detailed characteristics of VUF in CAP through calculations pertaining to an increasing stage that followed an initial steady state during transition to another steady state with higher rainfall intensity (Exp. 2) and a recession stage without rainfall following a steady state response to a constant rainfall (Exp. 3). Experiment 4 was added to examine the characteristics of VUF under

steady state conditions in response to rainfall with various constant intensities. The length of the soil column for experiments 1, 2, 3, and 4 was constant (70 cm). As shown later, the relationship of soil-column storage to the outflow rate during the recession stage was closely associated to a string of the relationships under steady state conditions. In addition, Experiments 5 and 6 were conducted to ascertain the meaning of parameter p in SFE as well as to identify dependences of VUF on soil-column depth. Evaporation was assumed to be negligible in all the experiments because our target was to examine only stormflow responses.

3. Experiment results

3.1. Comparison with field observations

The final stage of the 1987 storm observed at the SL shown in Fig. A4 was targeted for our comparison in Exp. 1 because this period can be estimated as a CAP due to enough amount of cumulative rainfall (see detailed description of this storm event in Appendix 1). Although comparisons focused on the responses in a CAP, calculations started at the onset of this July 14 storm: the initial condition of ψ was zero at the base of the soil column and the vertical distribution in the column was set at hydrostatic equilibrium. The results calculated by eight soil structures consisting of SA, SB, CR, LM, PF, LSA, KES, and SAB are shown in panels (a) to (h) of Fig. 3. The upper panels, (a1) to (h1), illustrate the observed rainfall intensity, r , the observed runoff rate, q_b , and the calculated outflow rate from the soil-layer bottom, u . The lower panels (a2) to (h2) show the observed and calculated ψ values at 10, 30, and 50 cm depths. The runoff rate, q_f , calculated by SFE with p and k of 0.3 and $27 \text{ mm}^{0.7} \text{ h}^{0.3}$, also plotted in Fig. A4, is inserted to the panel (a1).

Rapid propagation of the pressure head in the soil columns was commonly found in the observed and calculated values, and all the calculated hydrographs of outflow rates exhibited similar timescales to the storm runoff hydrographs observed in SL and calculated by SFE (Fig. 3). However, the magnitude of the delay and smoothing for the calculated results depended on the soil types, and the peak outflow rates in descending order were KES, LM, LSA, PF, SB, SAB, CR, and SA. The observed peak runoff rate and that calculated by SFE were almost the same and located between the peak outflow rates for CR and SA. Interestingly, LM, with the lowest K_s value, produced a high runoff peak although the highest K_s value was represented by PF. Hence, the outflow responses never reflected the magnitude of K_s , but were dependent on the hydraulic characteristics of VUF, which were controlled by relationships among ψ , θ , and K .

The calculated distributions of ψ for SAB in Fig. 3(h2) compared well with those observations, but this is obvious because this combination of these soils was tuned by a trial and error to get a comparatively good result. It should be rather noted that the local distributions of hydraulic variables were sensitive to soil hydraulic properties and stratified structures (Fig. 3, lower panels). A more important finding derived from this experiment was that temporal changes of u were rapid enough to produce the observed storm runoff response, regardless of soil structure.

The peak of each calculated outflow, with the exception of SA, was higher than the peak of the observed runoff, and its time of occurrence coincided closely to those observed for most of the soil structures (Fig. 3); however, both CR and SA exhibited a slightly later time of occurrence. Because the subsequent lateral flow was added to the VUF for hillslope runoff discharge, we have to consider an additional change of the hydrograph through lateral flow; nonetheless, these results suggest this change may be generally small (Fig. 3).

Some areas on the SL hillslope have very thin soil, and the unsaturated zone may become thinner than the depth of the soil layer near the hillslope toe because the accumulation of water there causes a rise of groundwater table. Consequently, these zones may contribute to the

generation of higher outflow peaks and earlier times of occurrence. Although effects of these heterogeneities on runoff responses are taken into consideration, it should be emphasized that the process of pressure-head propagation through the VUF (Fig. 3) can substantially contribute to the production of rapid storm runoff responses in a CAP. This occurs even though various flow components, including infiltration-excess and saturation-excess overland flows and preferential flow in the soil and weathered-bedrock layers may also contribute to the generation of storm runoff on a hillslope.

3.2. Summary of experiments with constant rainfall intensities

A large contribution of VUF to storm runoff responses was suggested from our comparison of the results from Exp. 1 with those observed on a hillslope. The next experiments attempted to further investigate the detailed distributions of hydraulic variables within a soil column and to elucidate whether the outflow rate produced through VUF can be generally approximated by the runoff rate (q_f) produced by the SFE. Consequently, Exps. 2 and 3 focused on responses to simpler rainfall conditions with constant intensities instead of conditions existing in a natural storm (i.e., Exp. 1).

Experiment 2 was conducted for a transient increasing stage from an initial steady state with a constant rainfall of 1 mm h^{-1} to a new steady state with a constant rainfall of 10 mm h^{-1} . This was selected as an example of hydrological responses to an increase in rainfall intensity during a CAP after the entire soil layer already became wet during large cumulative rainfall. Experiment 3 examined the recession stage after a steady state with constant rainfall of 10 mm h^{-1} .

Soil column length, soil type, and stratified structure in both Exps. 2 and 3 were the same as those for Exp. 1. Temporal changes in u calculated for each soil structure and changes in q_f calculated by SFE using the same parameter values as Exp. 1 are plotted in Fig. 4. Temporal and spatial distributions of hydraulic variables including ψ , θ , K , and downward flux (f_d) are illustrated in Fig. 5 to allow examination of the detailed hydrological behaviour in each soil column with different structures,

Fig. 6 shows the relationships of storage, S , to u , where S is defined as the storage (L) of the column of length of D (L):

$$S = \int_0^D \theta dz \quad (10)$$

S_d in Fig. 6(a) represents the storage of transient water, defined as:

$$S_d = S - S_0 \quad (11)$$

where S_0 is the storage at hydrostatic equilibrium with ψ at the column bottom of zero as:

$$S_0 = \int_0^D \theta(\psi = -z) dz \quad (12)$$

The S_f for SFE calculated from q_f in Eq. (1) is also plotted in Fig. 6(a). Fig. 6(b) shows the relationship in a log-log scale using the dimensionless ratio, S_* , of S_d to the total storage of transient water, defined as:

$$S_* = \frac{S_d}{S_s - S_0} \quad (13)$$

where S_s is the storage at full saturation of the soil column and defined as:

$$S_s = D\theta_s \quad (14)$$

Both S_* and u , the outflow rate from the soil-layer bottom, decrease toward zero because evapotranspiration is neglected in our numerical experiments, and the maximum of S_* is unity in response to the maximum of u , equal to K_s . Hence, this definition of S_* can provide a useful methodology for a comparison of the calculation results between VUF with SFE during the recession stage.

In addition to the results from Exp. 3, the values of S_* at steady state

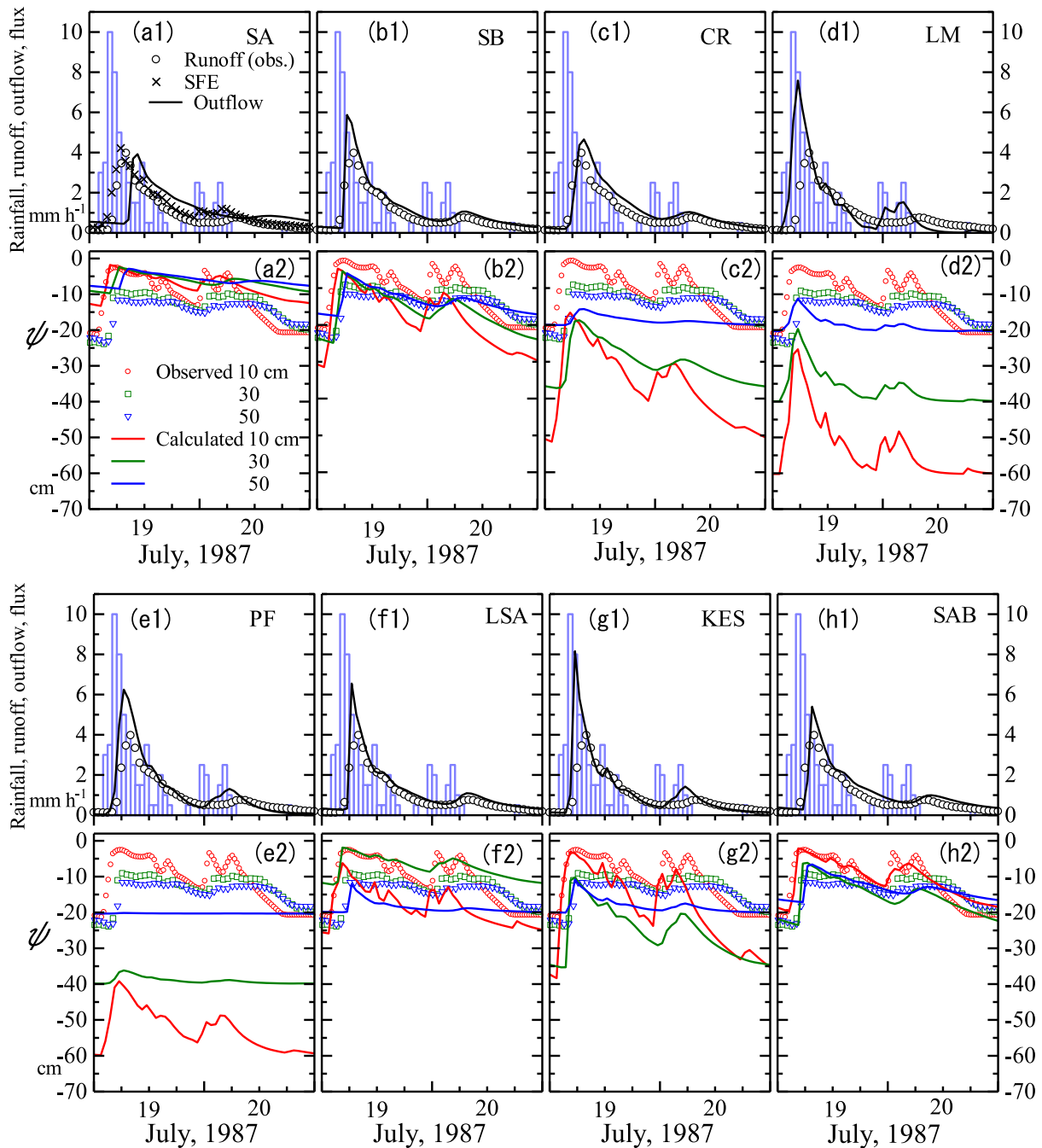


Fig. 3. Temporal changes for a storm event in July 1987 in the observed rainfall intensity, runoff rate at the SL, and the calculated outflow rate (panels a1 to h1), and temporal changes in the observed and calculated pressure head values at 10, 30, and 50 cm depths (panels a2 to h2). The runoff rate, q_f , calculated by SFE ($p = 0.3$ and $k = 27$) is inserted to the panel (a1). Symbol in each of panel a1 to h1 indicates the soil structure used in the calculation.

in response to a constant r intensity, obtained from Exp. 4, are plotted in Fig. 6(b). Lines inserted there are the gradients in the power law relationships between q_f and S_f given by p values in Eq. (1).

3.3. Increasing stage from an initial steady state to another with higher rainfall intensity

The order of increasing time at which outflow begins to increase (called hereinafter ‘increasing start time’) was LM, PF, KES, CR, LSA, SB, SAB, and SA (Fig. 4). However, the timing to approach a new steady-state rate of 10 mm h^{-1} differed due to differences in the rate of increase for each calculation: a relatively rapid increase is shown in the curves of KES, LSA, SB, SAB, and SA. In contrast, a gentle rate of

increase occurred in LM, PF, and CR. Hence, hydrographs may reflect differences in the pressure head propagation among various soil structures.

Effects of each soil structure on the distributions of variables, ψ , θ , and K and flux f_d are presented in Fig. 5. In the case of SA, where u increased rapidly, almost the entire soil column exhibited constant values of ψ , θ , and K except for a thin zone near the bottom when the column was under the initial and final steady states in response to the two rainfall intensities of 1 and 10 mm h^{-1} . In contrast, soil structure LM lacked zones with any constant values of these variables under both steady states, and increases in the values of these variables were smoothly transmitted from the surface to the bottom of the soil column, resulting in the early increasing start time of u (Fig. 4). However, the

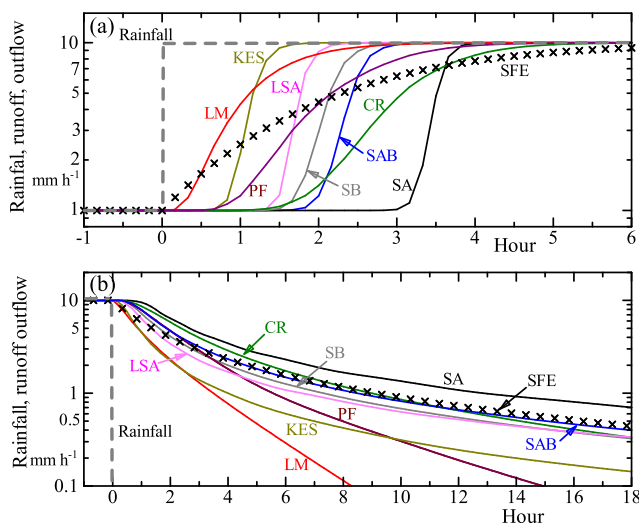


Fig. 4. Comparison between the runoff rate calculated by SFE with $p = 0.3$ and $k = 27$ and the outflow rates calculated by the numerical experiments with various soil structures. Panels (a) and (b) are the increasing and recession stages, respectively.

increasing curve for LM was much gentler than that for SA and the time when it attained the new steady state with 10 mm h^{-1} was not much different.

To understand the hydraulic behaviours that depend on soil hydraulic properties (as shown for SA and LM), we investigated the theoretical structure of Eq. (3) with a homogeneous soil structure. The effects of advection and diffusion on hydraulic behaviours are represented by the first and second terms on the right-hand side of Darcy's law (included in Eq. (3)) and rewritten from Eq. (5) as:

$$f_d \equiv -f = K + K \frac{\partial \psi}{\partial z} \quad (15)$$

Because the diffusion term is zero within the zone with constant hydraulic variables that was created in the upper portion of the soil column, the constant value of ψ is calculated from r by assigning r to K in Eq. (15). If the diffusion term can be negligible, the Richards equation in Eq. (3) is converted to the following continuity equation:

$$\frac{\partial \theta}{\partial t} \equiv C \frac{\partial \psi}{\partial t} = \frac{\partial K}{\partial z} \quad (16)$$

When rainfall intensity increases from r_1 to r_2 , the zone with flux r_2 is extended downward with velocity, v_a (Smith, 1983; Torres et al., 1998) and described as follows:

$$v_a = \frac{r_2 - r_1}{\theta(K = r_2) - \theta(K = r_1)} \quad (17)$$

When applying the equation to the VUF for SA, v_a is 18.7 cm h^{-1} because r_1 , r_2 , $\theta(K = r_1)$, and $\theta(K = r_2)$ are 1 mm h^{-1} , 10 mm h^{-1} , 0.338 , and 0.386 , respectively, and the propagation time for the 70 cm column was calculated as 3.7 h , suggesting the assumption of advection in Eq. (16) may be acceptable for SA (Figs. 4 and 5). Therefore, a large delay of the increasing start time of u in Fig. 4 was caused by a small value of v_a .

When each of the variables ψ , θ , and K are controlled only by the advection term, a sharp wetting front below the zone with constant values of hydraulic variables would be delineated as a horizontal line in each of panels (a) to (e) of Fig. 5. However, the actual wetting front in each panel was more or less smooth, caused by the diffusion term. Furthermore, the value of each hydraulic variable decreased with increasing depth along the wetting front. The distribution of ψ near the bottom of the column approached the hydrostatic-equilibrium line passing through $\psi = 0$ at the bottom, and the value of each variable

increased with increasing depth. Hence, the distribution of ψ has an inflection point at $\partial \psi / \partial z = 0$ between the two reverse curves (Fig. 5).

Consequently, the distributions of hydraulic variables in the soil column in an increasing stage can be segmented into three zones. The near-surface zone with constant values for the variables is controlled only by the advection term. The second and third zones are divided by the inflection point and both controlled by advection and diffusion terms. However, u does not begin to increase unless the inflection point of ψ departs from its original distribution under the initial steady state, where the downward flux, f_d , remains equal to the initial outflow rate of 1 mm h^{-1} . Therefore, for soil types such as SA where a large rainwater is absorbed in the first and second zones, the inflection point departing from the original distribution is deep, and the increasing start time of u is late (Figs. 4a, 5a1). After the inflection point departs from its original distribution, the increase of ψ at the inflection point is transmitted to the bottom due to an effect of the diffusion term, and u rapidly increases from the initial rate to the final steady state.

On the other hand, for soil types such as LM (Fig. 5d1) where the near-surface zone controlled by the advection term is hardly produced, the inflection point of ψ created at a shallow depth rapidly departs its original distribution. Hence, u rapidly begins to increase but the increasing velocity is low because most of the rainwater supplied from the surface is allocated to storage increase throughout the soil column and only a small portion of the storage increase is discharged as u (Figs. 4a, 5d2). Accordingly, the interdependence between u and storage volume may cause a gradual increase of u . Indeed, Fig. 4 demonstrates that the runoff rate, q_f , calculated by SFE, was the most gradual increase, because a large portion of the rainwater was allocated to storage, S_f , from the beginning of increasing stage due to the one-to-one relationship between q_f and S_f in Eq. (1).

Consequently, the VUF in the increasing stage during a CAP may produce a different outflow response from the storm runoff response calculated from SFE because a delay for the increasing start time of u is created in the former but not in the latter. Nonetheless, the total time necessary for outflow increase is enough short and similar to that for storm runoff responses not only calculated by SFE but also observed on a hillslope (Figs. 3 and 4). However, the short timescale similar to storm runoff responses is generated only during CAPs but much longer timescale is needed when the initial soil condition is dry. This issue will be discussed in Section 4.1.

Next, let us compare the behaviours of VUF and their contributions to the outflow responses among soil types. Fig. 6a shows that the increase of S_d for each soil type is constructed of two portions represented by a dashed line and dashed-dotted line. The former represents a vertical line without an increase in u because the inflection point of ψ has not yet departed from its original distribution under the initial steady state. On the other hand, the latter represents an inclined curve because the inflection point has already departed from the original distribution and the storage increase is accompanied by an increase in u . The increasing patterns of u for the homogeneous soil structures in Fig. 4 are explained by the distributions of volumetric water content in Fig. 5 as follows: the earlier increasing start time for SB compared to SA is caused by its smaller difference of θ between the two steady state conditions (panels a2 and b2), resulting in a larger v_a in Eq. (17). A comparatively shallow inflection point of ψ (panel e1) for PF coincided with a gentle increase of u in Fig. 4. The curve of u in CR in Fig. 4 with a late increasing start time and a gentle curve may result from the distribution pattern where the inflection point of ψ departs from the original distribution at an intermediate depth (panel c1).

Unlike homogeneous soil structures, the distributions of hydraulic variables ψ , θ , and K for stratified structures in panels (f) to (h) of Fig. 5 were complex, particularly near the borders between layers. In both homogeneous and stratified structures, however, it should be noted that the downward flux, f_d was constant or monotonically decreased with increasing depth throughout the transient process from one steady state to another in response to increasing rainfall intensity. Consequently,

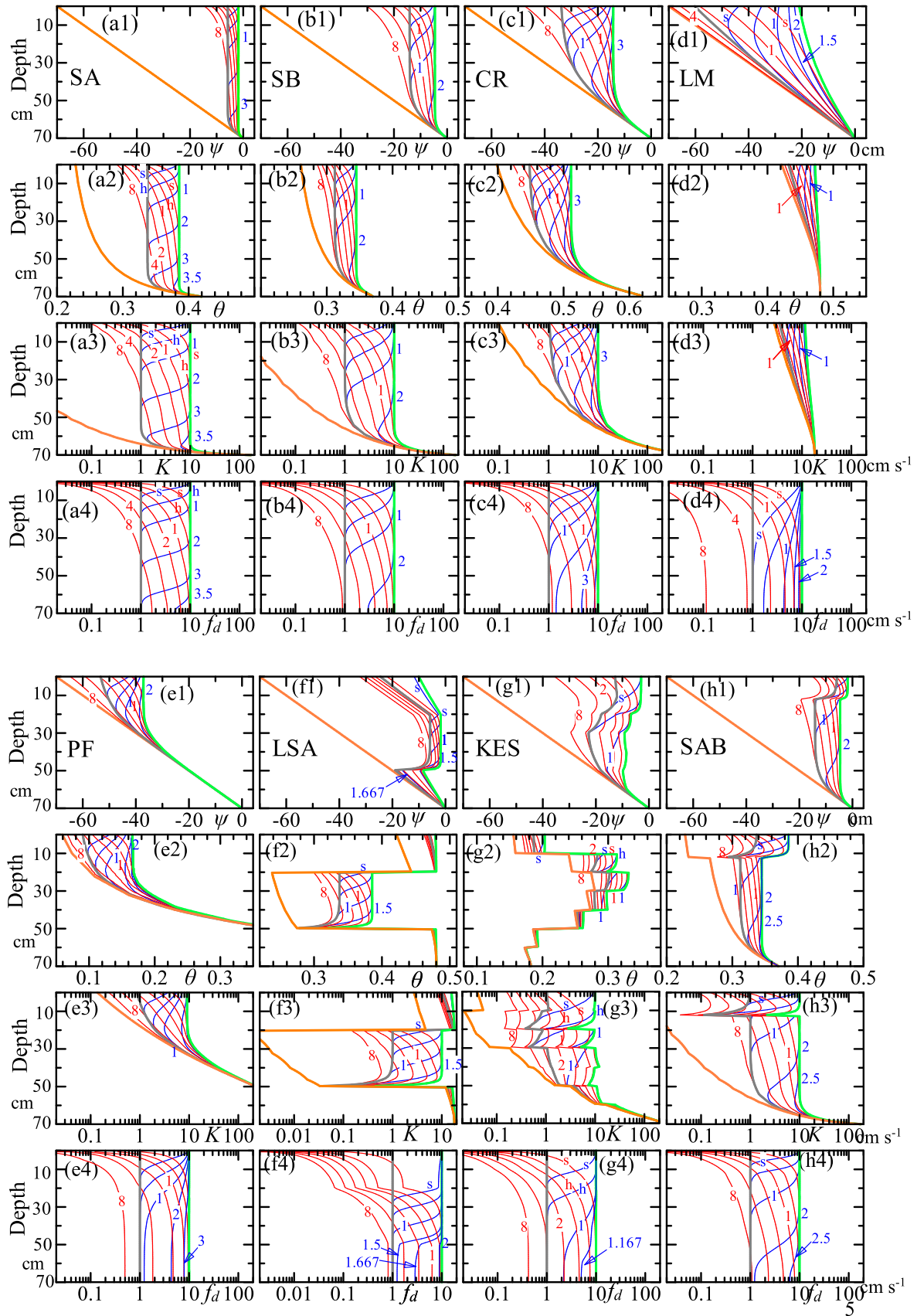


Fig. 5. Changes in the distribution of ψ (a1–h1), θ (a2–h2), K (a3–h3), and f_d (a4–h4) in the increasing (blue lines) and recession stages (red lines) for the eight types of soil structures in the column. Orange thick line: hydrostatic equilibrium. Gray thick line: steady state with $f_d = 1 \text{ mm h}^{-1}$. Light-green thick line: steady state with $f_d = 10 \text{ mm h}^{-1}$. Number in each panel indicates the elapsed time (hour) from the beginning of each experiment, and symbols s and h indicate 10 and 30 min from the start, respectively.

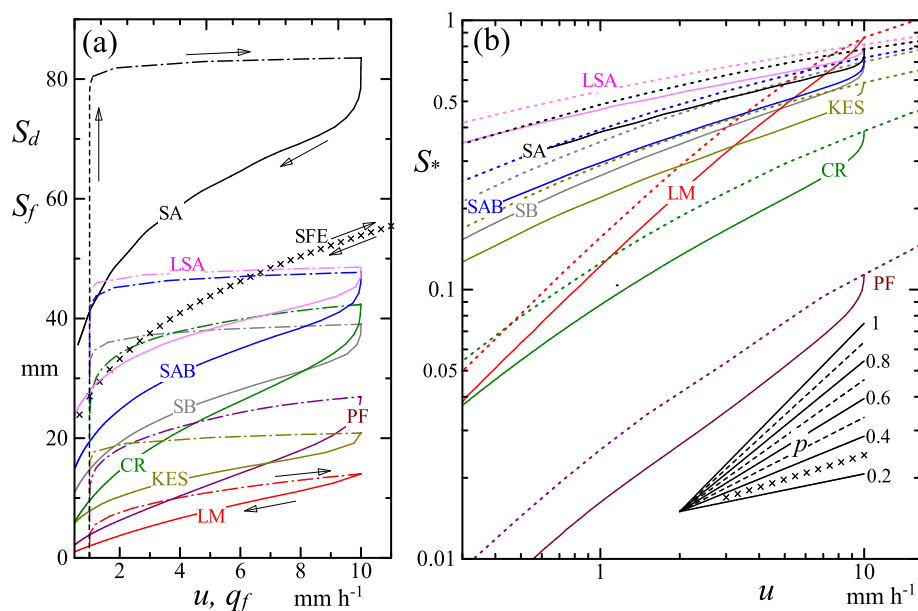


Fig. 6. Relationships of storage to outflow rate for the soil column with those of watershed storage to runoff rate calculated by SFE. (a): The storages S_d and S_f are respectively plotted against u and q_f in a normal scale. Dashed line and dashed-dotted line show the u - S_d relationship in the increasing stage without and with increase of u , respectively, and solid line shows that in the recession stage. Relationship between q_f - S_f is plotted by crosses. (b): The dimensionless storage S^* is plotted against u in a double logarithmic scale. Solid line shows the u - S relationship in the recession stage. Dotted line shows the string of relationships under steady states with various constant rates of u . Lines on the bottom-right corner show the gradients of power law functions with various p values, although the function with $p = 0.3$ is specified by crosses.

smooth curves of f_d compared to the hydraulic variables are illustrated in each of the bottom panels (f4) to (h4) of Fig. 5. Therefore, even though the distributions of variables were varied considerably, we believe that their complex shapes resulted from the calculation processes (i.e., Eq. (3)), which ensured that smooth distributions of f_d are produced from the boundary conditions.

For KES, the propagation time calculated from v_d was 1.36 h, shorter than that for SA, SB, and SAB. This may be caused by the soil structure, consisting of soils with relatively small differences between θ_r and θ_s (Fig. 2 and Table 1c), responding to an early increase of u (Fig. 4). The distribution for soil column LSA exhibited an interesting shape due to an immediate transmission in the both side layers with LM and a delay of the transmission was mainly created in the SA layer sandwiched between the LM layers (Fig. 5f2). Hence, the delay in the transmission through the 30 cm SA zone was calculated as 1.6 h (Eq. (17)), matching the timing of the increasing start time for LSA in Fig. 4.

From the distributions of hydraulic variables for three stratified structures (Fig. 5f to h), it is apparent that the downward fluxes (f_d) were similar to those found in the homogeneous soil structures. Consequently, we suggest that the dependences of u on the behaviours of VUF may be generally applicable, irrespective of whether soil hydraulic properties in the column are homogeneous or heterogeneous.

3.4. Recession stage from a steady state

At the beginning of the recession stage, time was required for the transmission of a sudden flux change at the soil-layer surface to the bottom (Fig. 4). This is represented by each curve in both panels of Fig. 6, which exhibited a small region showing a storage decrease accompanied with little decrease of u at the beginning of recession stage. However, each curve in Fig. 6 was soon connected to a smooth curve with an intrinsic outflow and storage relationship.

Because the surface boundary condition changed from constant rainfall intensity to zero at the beginning of Exp. 3, f_d always increased with increasing depth throughout the recession stage. When soil hydraulic properties were homogeneous (panels [a] to [e] of Fig. 5), the variables ψ , θ , and K increased monotonically with increasing depth. These monotonic increases may be reflected in smooth decreasing curves of u without abrupt changes in Fig. 4 and smooth curves of the distributions of the variables without inflection points in Fig. 5. Although the increasing start time and inflection point were created in an increasing stage (Section 3.3), the entire column in a recession stage

was always included within the zone controlled both by advective and diffusive terms of Eq. (15). Consequently, Fig. 6 shows that relationships between outflow and storage exhibited smooth curves throughout the recession stage, and that the gradients of these curves were comparable with the gradient controlled by parameter p of SFE.

The outflow and storage relationships in the dimensionless scale in Fig. 6(b) demonstrate that all curves in the recession stage from Exp. 3 were parallel to those in a string of relationships under steady-state conditions obtained from Exp. 4 (except near the beginning of the recession stage). The parallel curves for all soil structures were slightly upwardly convex and their gradients increased with decreasing outflow rates.

Comparing responses among the five homogeneous soil structures, those producing late increasing start time of u , arising from the effect of the near-surface zone controlled only by the advection term in the increasing stages (e.g., SA and SB), tended to have smaller p values in the recession stage, whereas those structures characterized by gradually increasing curves (e.g., LM and PF) had larger p values. Intermediate p values were detected for CR, which produced an intermediate curve characteristic for u . Such dependences of p value on soil hydraulic properties are examined in Exps. 5 and 6 in Section 3.5.

For each of the three stratified soil structures (LSA, KES, and SAB), the increase in f_d with increasing depth (Fig. 5f4–h4) was similar to that for each of the homogeneous structures even though those for ψ , θ , and K for each stratified structure were considerably deformed near the layer junctions. Such a low sensitivity of f_d to heterogeneities is reflected in their similar shapes compared to those with homogeneous properties both in hydrographs (Fig. 4) and in the outflow-storage relationships (Fig. 6). Therefore, it is noted that the outflow-storage relationship can be approximated by a power-law equation in SFE even though the soil structure is heterogeneous.

3.5. Parameterization of vertical unsaturated flow for the runoff-storage relationship

In order to determine dependences of p values included in SFE on soil hydraulic properties and soil column lengths, additional numerical experiments (Exps. 5 and 6) were conducted for soil columns with hydraulic properties of SB. Experiment 5 focused on a recession stage similar to Exp. 3, although the length of the column and the flux intensity for the initial steady state conditions were set as 200 cm and 100 mm h⁻¹, respectively. Experiment 6 was similar to Exp. 4 for a

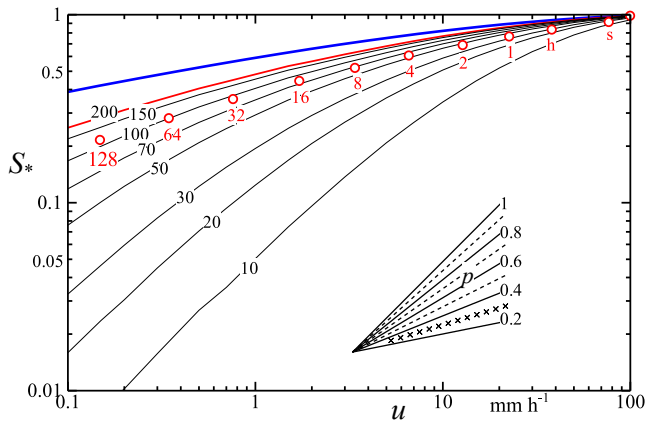


Fig. 7. Comparison of dimensionless storage, S_* , to outflow rate, u , among soil columns of different lengths with hydraulic properties of SB. Black line is the string of relationships under steady states with various constant rates of u (Exp. 6), and number by the line is the column length (cm), although the string of relationships in the 200-cm column is specified by a red line. Red circle is the relationship in the recession stage from the steady state with u of 100 mm h^{-1} in the 200 cm column (Exp. 5). Number by each of the circles indicates the elapsed time (hour) from the steady state, and the meanings of s and h are the same as in Fig. 5. Blue line indicates the θ - K base relationship. Lines and crosses at the bottom-right corner are the same as in Fig. 6.

string of the steady-state responses of VUF to various rainfall intensities, but the calculations were made for eight columns with lengths, D , of 10, 20, 30, 50, 70, 100, 150, and 200 cm.

The relationships of S_* to u calculated from the experiments are illustrated in Fig. 7. The relationship between u and S_* directly calculated from the hydraulic properties K and θ for SB (hereinafter called the θ - K base relationship) is also plotted in Fig. 7 by substituting steady-state flux, u , into K and converting θ to S_* using Eqs. (6), (10)–(13). Fig. 8 shows the distributions of θ in the 200 cm soil column at several time points during the recession stage (Exp. 5) and those under the steady-state conditions (Exp. 6) producing the same u value as in the recession stage.

The vertical distribution of θ for steady-state conditions obtained from Exp. 6 was generally segmented into two zones (Fig. 8): vertical lines near the surface were originated from the advection term of

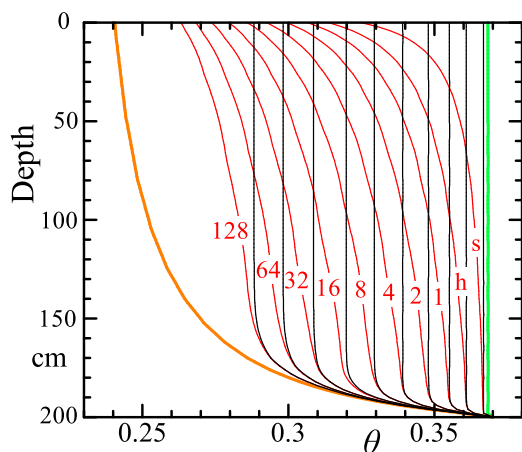


Fig. 8. Comparison of the distributions of volumetric water content under steady-state (black line; Exp. 6) and in the recession stage (red line; Exp. 5) for a soil column with a length of 200 cm. Orange thick line: hydrostatic equilibrium. Light-green thick line: steady state with $f_d = 100 \text{ mm h}^{-1}$. Numbers by lines in the recession stage indicate the elapsed time (hour) from the steady state, and the meanings of s and h are the same as in Fig. 5.

Darcy’s law in Eq. (15), and K values along these lines were regarded equal to the downward steady-state flux, f_d , and rainfall intensity, r , because $\partial\psi/\partial z = 0$ in Eq. (15). On the other hand, our bottom boundary condition $\psi = 0$ enforced higher K values than f_d and values of $\partial\psi/\partial z$ close to -1 in Eq. (15) near the bottom. Consequently, both distributions in the recession stage and under steady-state conditions approached hydrostatic equilibrium near the bottom. The former zone near the surface and the latter zone near the bottom are hereinafter defined as an ‘advection zone (AZ)’ and an ‘asymptotic equilibrium zone (EZ)’, respectively.

The gradients of u - S_* relationships were then examined. The θ - K base relationship can be regarded as the u - S_* relationship for a very long soil column (Fig. 7) where the proportion of EZ to the total column length is negligible because most of this column is within AZ (Fig. 8). Therefore, u - S_* curves under steady-state conditions approach the θ - K base relationship as column length increases (Fig. 7); thus, we recognize that the smallest p value in response to a given range of u is determined by the θ - K base relationship derived from soil hydraulic properties.

In contrast to long columns, the u - S_* relationships for short columns exhibited large p values approaching unity, indicating the linear relationship between u and S_* , as column length decreased (Fig. 7). This may reflect the distribution of θ under steady-state conditions (Fig. 8): the distribution of a steady-state flux is controlled only by the bottom boundary condition but not dependent on the column length. Consequently, the steady-state distribution of θ illustrated for depth from the bottom (200 cm) to $200-D$ cm (Fig. 8) may represent the distribution of θ for the soil column with length of D , and almost the entire portion of a column with a very small D value may reside within EZ. For the soil hydraulic properties of SB, therefore, the range of p may range from unity for a short column residing mostly in EZ to a small value for a long column derived from AZ (Fig. 7).

Interestingly, this dependence of p on the proportion of the AZ and EZ zones is also detected in the dependence on the hydraulic properties in each homogeneous soil (Fig. 6). For example, Fig. 5(d2) shows most of the column LM was covered within EZ or a transition zone between EZ and AZ under steady-state conditions with $u = 1$ or 10 mm h^{-1} , but vertical lines representing AZ were not contained in the steady-state distributions. These distributions may be reflected in the value of p for LM (Fig. 6b), that is, $p \approx 1$ for $u = 1 \text{ mm h}^{-1}$ and a slightly smaller p value for $u = 10 \text{ mm h}^{-1}$. On the other hand, Fig. 5(a2) shows that most of the column for SA was covered with AZ under the steady state, resulting in the smallest value of p for a local u value in Fig. 6(b). The slightly higher p value for SB compared to SA can be explained by the shorter AZ for SB (compare Fig. 5b2 and a2).

Consequently, we can conclude that dependences of p values on soil hydraulic properties and soil column lengths are mainly controlled by the vertical distribution of θ in a column with a given length under a steady-state condition. Because this distribution may be controlled by the soil pore-size distribution in Eqs. (6) and (7) (Kosugi, 1996) and ψ_m is incorporated as a parameter originated from the median pore radius, a dimensionless parameter, δ , was introduced here to parameterize the characteristics of vertical unsaturated flow for the p values.

$$\delta = -D/\psi_m \tag{18}$$

Fig. 9 shows the dependence of p on δ in response to $u = 1 \text{ mm h}^{-1}$ based on the results of Exp. 6. Eight plots for SB and a plot for each of other four soil types indicate the results for columns with lengths from 10 to 200 cm and the result for the 70 cm column, respectively. Besides, p values for the θ - K base relationships of these soils are also plotted at the right side. Although soil hydraulic properties and column length both involve the dependence, the decreasing tendency of p from 1 to a small value given by the θ - K base relationship can be consistently detected in response to increasing δ value.

Accordingly, δ may play an important role in the hydraulic behaviours of VUF. Such a dimensionless parameter defined as a ratio of vertical soil-column length to representative pressure head was often

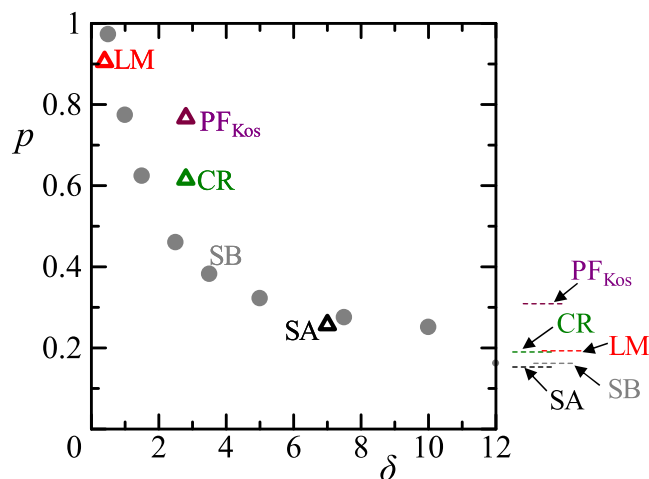


Fig. 9. Dependence of p on δ in response to $u = 1 \text{ mm h}^{-1}$ based on the results of Exp. 6. Eight plots for SB (gray circle) and a plot for each of other four soil types (triangle) indicate the results for columns with lengths from 10 to 200 cm and the result for the 70 cm column, respectively. Dashed line at the right side indicates θ - K base relationship for each soil.

introduced by similarity analyses of unsaturated flow (Miller and Miller, 1956; Verma and Brutsaert, 1970; Tani, 1982, 1985b). However, the basic hydraulic findings from these studies have been rarely used for the hydrological studies on storm runoff response (Tani, 1985a; 2013). It is believed that our finding on parameterization of VUF for the relationship of p to δ may contribute to a new perspective about a coupling of hydrology with soil physics.

4. Discussion

4.1. Effects of soil wetness on outflow response

Our numerical experiments strongly suggest that VUF may produce rapid outflow responses to storm rainfall regardless of the type of soil structure as long as the entire soil layer is already wet in a CAP. This suggests the lateral flow, receiving outflow from the vertical flow process, is so fast that storm flow hydrograph is little deformed through the lateral process in a CAP. We first discuss the rationale why such rapid responses were produced from VUF.

The interdependence of outflow and storage was detected in the increasing stage from one steady state to another only after the inflection point of ψ departs from its original distribution under the initial steady state (Fig. 5), resulting in a creation of increasing start time of u (Fig. 4). However, the timescale of this increasing start time is significantly different between wet conditions during CAP and dry conditions prior to a rainfall event.

Note that the usual range of rainfall intensity, r , from 1 mm h^{-1} for a very gentle intensity to 100 mm h^{-1} for an extraordinarily heavy storm is limited small compared to the full range of unsaturated hydraulic conductivity, K , and that this may cause large effects of soil wetness on the outflow responses. Because sufficient cumulative rainfall occurs from the start of the event during a CAP, the range θ at every depth of the soil column is included only in a small wet portion of the full range from θ_s to θ_s . This small fluctuation range of θ results in a large v_a (Eq. (17)) and may explain why the VUF during a CAP can produce a rapid runoff response with an early increasing start time. Such a rapid response was observed not only in our study hillslope, SL, (Fig. A4) but also in a small unchanneled watershed, CB1 (Torres et al., 1998; Ebel and Loague, 2008).

On the other hand, we should note that K values for dry soils prior to a rainfall event are several orders of magnitude lower than those during a CAP because of the effects of evapotranspiration and infiltration

during the previous rainless period. Consequently, remarkably different behaviours are produced from the VUF under different wetness conditions due to the nonlinear relationship of K to θ : much rainwater at the beginning of an event is absorbed when the soil column was dry, whereas most of the rainwater received during a CAP rapidly contributes to outflow even though its increasing start time may be created.

This large effect of soil wetness on VUF clearly explained the characteristics of the relationships between total storm rainfall and runoff SL and MN (Fig. A2), which were composed of a dependence of storm runoff volume on the initial runoff rate and a large allocation of rainwater volume to storm runoff volume after large cumulative rainfall. Accordingly, threshold responses discussed by previous studies (Noguchi et al., 1997; Tani, 1997; Graham and McDonnell, 2010; Ali et al., 2013; Dusek and Vogel, 2016) may, at least partly, be explained by the hydraulic behaviours of VUF, as discussed here.

4.2. Sensitivity of outflow response to spatial heterogeneities

Next we discuss the dependency of outflow response on spatial heterogeneities that characterize a natural hillslope soil. To address this, it is important to understand differences in hydraulic characteristics between lateral and vertical water flow systems in the soil.

Groundwater flow in the saturated zone plays a main role in the lateral-flow system contributing to storm runoff response (Tani, 2008; Dusek et al., 2012). Because all the pores included in the soil are filled with water due to the positive pressure potential in the saturated zone, flow velocity is mainly controlled by large pores with small friction resistances. Even though most of the soil layer is occupied by the soil matrix, flow through a preferential path may play a dominant role in the lateral system, where this exists. Particularly, we should note the large difference in the position of the groundwater table during a CAP: the soil layer without preferential paths may contain a substantial saturated zone due to a large rise of water table in response to heavy rainfall, whereas the unsaturated zone coupled with a low water table remains in the layer containing preferential flow paths because of the effective drainage of groundwater through them.

The hydraulic behaviour in many preferential pathways cannot be described by Darcy's law but rather by the Manning equation, previously derived from measurements of undisturbed soil with natural pipes (Kitahara, 1993) and hydraulic experiments using artificial pipes (Sidle et al., 1995; Tsutsumi et al., 2005). However, the spatial distribution of K_s in the soil matrix and the resistance for a preferential flow network are very difficult to estimate due to their large heterogeneous distribution. This causes a fundamental problem for evaluating the effects of lateral flow on runoff response because the velocities through preferential flow networks range across several orders of magnitude (Anderson et al., 1997; Uchida et al., 2003).

Hence, although many observational studies suggest that storm runoff responses were produced through the lateral flow system, including preferential flow paths (McDonnell, 1990; Sidle et al., 2001; Uchida et al., 2005; Guo et al., 2014), these individual findings can be hardly extended to a general quantification about the roles of the lateral system. This is because of the unknown spatial distribution of these paths. Indeed, it is extremely difficult to formulate the necessary generality required for modelling processes within a soil with abundant heterogeneities, unlike a homogeneous system (Sidle et al., 2001; McDonnell et al., 2007; Troch et al., 2009).

Effects of the heterogeneities on the VUF may be significantly different from those impacting lateral flow systems. Connecting paths around living or decayed tree roots certainly produce a quick bypass flow in the unsaturated zone (Noguchi et al., 1999; Liang et al., 2011; Ghestem et al., 2011), but the contribution of rapid flow through them may be insufficient to allow a large volume of storm runoff that is nearly equivalent to the rainfall volume in a CAP. The soil matrix surrounding these paths may also play a role in the production of the large runoff volume (Tsuboyama et al., 1994). In addition, our analysis

on VUF has demonstrated that the propagation of ψ within the soil matrix in a CAP has enough impact to produce a quick storm response (Figs. 4 and 5). The effects of heterogeneity on VUF are examined next, based on an application of soil physics.

Let us consider a storage change in an unsaturated zone in response to a change in the vertical flux. This process follows the continuity equation derived from Eqs. (3) and (15) as:

$$\frac{\partial \theta}{\partial t} = \frac{\partial f_d}{\partial z} \quad (19)$$

Hence, a temporal change in θ in a local thin horizontal layer within the unsaturated zone generally arises in response to a change in f_d ($L T^{-1}$) passing through it, as long as the layer is under a non-steady state. Because such a change from θ to $\theta + \Delta\theta$ occurs at every local layer, the local change is extended to a change in storage of a large portion of the soil column.

Such an interdependence between θ and f_d does not occur before the inflection point of ψ departs from its original distribution under an initial steady state (Fig. 5). Because this isolation of the surface zone from the layer bottom does not occur during a recession stage, however, it should be emphasized that the interdependence at a local point may strongly support a close relationship of u to the total storage in the entire soil column approximated by SFE as shown in the u - S relationships (Fig. 6b).

Note that this interdependence is derived from $\Delta\theta$ at each local point in the soil column during a recession stage. Then, the effects of heterogeneities can be easily understood: because water is preferentially retained smaller pores by capillary forces compared to larger ones in an unsaturated zone, θ can be described by the relationship $C(-d\theta/d\psi)$ as the pore capillary pressure distribution function (Kosugi, 1994), and thus:

$$\theta(\psi) = \int_{-\infty}^{\psi} C(\psi) d\psi \quad (20)$$

Because this equation may be generally applied to any soil, even for PF with a small amount of fine particles, the dependence of the storage change in the entire soil column on $\Delta\theta$ occurs in all soil types. This common characteristic found in an unsaturated zone is particularly important because the outflow rate and the entire column storage are always interdependent whether the distribution of soil hydraulic properties is homogeneous or not, causing that the sensitivity of the interdependence to heterogeneities of soil structure may be generally small. This is because preferential paths with large pores that characterize heterogenous soils, may play only a limited role in the VUF due to their small capillary forces, unlike the lateral flow system.

We can therefore conclude that the approximation of storm runoff responses by SFE may be commonly acceptable by regarding the VUF as the main mechanism of stormflow generation, irrespective whether the soil structure is homogeneous or heterogeneous.

4.3. Connection between vertical and lateral flow processes

Vertical flows both in the soil matrix and via preferential paths can produce storm runoff responses (Fig. 1). In a CAP, however, a large magnitude storm runoff must be produced through lateral flow processes from water provided by vertical flow throughout almost the entire slope area. Because our findings from this paper are limited only to vertical processes, it has not been demonstrated what downslope-drainage processes produce large-magnitude storm runoff responses in CAPs. However, some field studies showed that rainfall-runoff responses were mainly produced through VUF and lateral flow process gave little deformation to storm flow hydrograph.

Although characteristics of storm runoff responses are qualitatively similar between the watershed MN and the hillslope SL in Tatsunokuchi-yama Experimental Watershed (see Appendix 1), the geometry of 96% of the area in MN is different from that of SL. Instead of

a thin soil layer overlying a hard quartz porphyry bedrock at SL, hillslopes in MN generally have deep weathered Paleozoic sedimentary bedrock, and most rainwater infiltrates into this deep zone. A recent study by Hosoda and Tani (2016) monitored the responses of the groundwater table in the weathered bedrock including the formation of clays and joints, on a general hillslope in the MN (see the location in Fig. A1), demonstrating that the water table quickly rose and fell after the entire soil layer became sufficiently wet. In such wet conditions, an analysis of SiO_2 concentration showed more than half of the stream water was occupied by pre-event water.

The volume of storm runoff for MN was almost the same as that of rainfall in CAPs (Fig. A2). During these wet periods, the conversion of hyetograph to the hydrograph might be created through vertical flow processes because the hydrograph responses were mostly synchronized with groundwater-table responses (Hosoda and Tani, 2016). Such synchronization cannot be explained unless fissures in the bedrock played a role in groundwater drainage as noted in another watershed underlain by sedimentary bedrock (Onda et al., 2001).

Another field study in a small steep watershed in the Rokko Mountains, Japan was conducted based on observations from numerous wells in weathered granite bedrock (Kosugi et al., 2011). This study showed triple-peak runoff responses at different timescales controlled by groundwater in two regionalized bedrock aquifers and the soil-mantle groundwater, although most mountainous watersheds do not show such multiple-peak runoff responses. Kosugi et al. suggested that these unique hydrological processes might be affected by diastrophic activities producing many fault lines. The synchronization of responses between the groundwater-table and stream water may support our argument on the flow mechanism: although a large lag time for each of the two slower runoff peaks is not in the range of stormflow responses, the results at this site can be understood by our concept that the conversions of hyetograph to hydrograph might be mainly created not through lateral flow processes but through vertical flow processes.

Based on the results obtained from watershed and hillslope observations previously described, as well as from our numerical experiments, we conclude that vertical flow component, not lateral one, may play a dominant role in the conversion from the hyetograph to hydrograph in a CAP (see Fig. 1), although the spatial scale involved in vertical processes is generally much shorter than for lateral flow processes. This tendency provides a novel point for physically-based storm-runoff models because the rainfall-runoff responses may depend more strongly on properties involved in vertical flow than those for lateral flow. Indeed, Montgomery and Dietrich (2002) showed that the time lag between rainfall and runoff for a steep hillslope depended little on slope gradient but was rather controlled by the soil moisture retention curve, suggesting a larger contribution of VUF to rainfall-runoff responses.

Some studies proposed runoff models treating VUFs independently from the total runoff processes on a hillslope (Ohta et al., 1983; Tani, 1985a; Dusek et al., 2012) although vertical preferential flow and lateral flow system may also be involved in storm runoff responses as shown in Fig. 1. Our discussion above may suggest a rationality in these models. Certainly, dependences of storm runoff responses on watershed properties might emerge from more sophisticated models based on the three-dimensional form of the Richards equation (VanderKwaak and Loague, 2001; Sudicky et al., 2008; Mirus and Loague, 2013). Nonetheless, we should note that preferential paths constructed of large pores work in effective lateral drainage routes insofar as they are included in the saturated zone (Section 4.2). This effect, derived from strong spatial heterogeneities, suggests a serious limitation to any kinds of models based on the Richards equation, because the modelling method representing such severe heterogeneities has yet to be developed (Montgomery and Dietrich, 2002; Uchida et al., 2005; Ebel et al., 2007; Chiffard et al., 2019).

Consequently, storm runoff models not only focusing only on vertical processes, but also describing the three-dimensional processes,

suffer from similar problems related to quantifying the effects of heterogeneous preferential flow networks on storm runoff responses. A next stage of the runoff model development must specify each effect of the vertical and lateral processes on the responses.

Our study has demonstrated that storm runoff responses in a CAP approximated by SFE can be roughly explained by VUF although the effects of the subsequent lateral flow on the hyetograph-hydrograph conversion may not be addressed. Probably, preferential paths provide rapid lateral drainage of groundwater (Anderson et al., 1997; Montgomery and Dietrich, 2002; Dusek et al., 2012), resulting in a small contribution of the lateral flow to hydrograph change. However, it is a fundamental question whether such a rapid drainage generally occurs on a steep hillslope.

We assume that subsurface structures including preferential paths are developed through long time-scale processes: field investigations for steep hillslopes in tectonically active regions have suggested that the subsurface structures producing runoff processes may have evolved through geomorphological processes supported by vegetation effects (Shimokawa, 1984; Heimsath et al., 1999; Roering et al., 2002; Istanbuluoglu and Bras, 2005; Matsushi and Matsuzaki, 2010, Sidle and Bogaard, 2016). However, the support of vegetation root system is not sufficient to maintain slope stability for this long period against often occurrences of large-magnitude storms because a rise of the groundwater table often triggers a landslide occurrence (Montgomery et al., 2009; Milledge et al., 2014; Boggard and Greco, 2015).

Consequently, it is needed to restrain the rise of the groundwater table by the effective drainage of groundwater preferential flow paths (Tani, 2013; Matsushi et al., 2016; Watakabe and Matshushi, 2019). Further interdisciplinary studies are needed to understand a connection between a short-timescale hydrological process producing storm runoff responses and a long-timescale geomorphological process creating the subsurface structures.

5. Conclusions

Hydrological studies on flood control suggest that the storm runoff response to rainfall in quasi-steady-state periods, when a large constant portion of rainfall is allocated to storm runoff, could be simulated by a simple runoff model based on a power-law equation between runoff rate and watershed storage. Our paper examines why this model produces good results using numerical experiments with the one-dimensional vertical form of Richards equation. The findings are summarized as follows:

- 1) The propagation of the pressure head through vertical unsaturated flow could produce a rapid response in the outflow rate from the bottom boundary of the soil column similar to storm runoff response observed on a hillslope, regardless of soil hydraulic properties.
- 2) Vertical distribution of pressure head in the soil column during an increasing stage from an initial steady state to another with higher rainfall intensity was characterized by the creation of an inflection point below the wetting front, above and below which the pressure head decreased and increased with increasing depth, respectively: the shape of outflow hydrograph was controlled by the depth where the inflection point departed from its original distribution under the initial steady state.
- 3) Although the delay of increasing start time of outflow rate in an increasing stage was small enough to produce rapid storm runoff responses during a quasi-steady-state period, the absorption of rainwater within dry soil did not usually contribute to storm runoff response at the beginning of a rainfall event. This could partly explain the so-called threshold storm-runoff response.
- 4) The outflow rate and the total storage in the entire soil column were interdependent throughout the recession stage. The outflow-storage relationship was approximated by a simple power-law equation, and

such an approximation was originated from a string of relationships of the total storage to constant outflow rate under steady-state conditions.

- 5) The exponent of the power-law equation reflected the distributions of hydraulic variables in the soil column and was controlled by a ratio of vertical soil-column length to representative pressurehead: the exponent ranged from unity, linear outflow-storage relationship, for a small ratio to the smallest value for a large ratio, originating from the relationship between hydraulic conductivity and volumetric water content for the given soil.
- 6) The reason why the outflow rate and the entire column storage are interdependent was derived from the characteristic of the unsaturated zone, where water is preferentially retained in smaller soil pores with large capillary forces compared to larger ones. This interdependence occurs irrespective of whether the distributions of soil hydraulic properties are homogeneous or not, resulting in a low sensitivity of outflow response to soil heterogeneities. This may provide a rationale for applying simple runoff models to storm runoff responses.
- 7) Because every runoff model representing three-dimensional processes on a hillslope suffers from problems related to quantifying the effects of heterogeneous preferential flow networks on storm runoff responses, a next stage of the runoff model development must specify each effect of the vertical and lateral processes on the responses in consideration of the heterogeneities.

Large dependences of storm-runoff responses on vertical unsaturated flow processes estimated from this study may encourage the development of innovative physically-based runoff models. This may also suggest the need for future interdisciplinary studies consisting of hydrology and geomorphology to ascertain characteristics of heterogeneous lateral flow systems in steep hillslopes.

CRediT authorship contribution statement

Makoto Tani: Conceptualization, Methodology, Writing - original draft, Writing - review & editing. **Yuki Matsushi:** Conceptualization. **Takahiro Sayama:** Methodology. **Roy C. Sidle:** Writing - review & editing. **Nagahiro Kojima:** Validation.

Declaration of Competing Interest

The authors declare that they have no known competing financial interests or personal relationships that could have appeared to influence the work reported in this paper.

Acknowledgements

We wish to thank valuable comments from Murugesu Sivapalan, Jeffrey J. McDonnell, Arjun M. Heimsath. This paper is a main product of a research project supported by the Japan Society for the Promotion of Science (JSPS) for KAKENHI grant number 23221009, titled "Prediction of catchment runoff changes based on elucidating a nested structure consisting of the developments of topography, soil, and vegetation." We appreciated the members: Ken'ichirou Kosugi, Hikaru Kitahara, Ikuhiro Hosoda, Taro Uchida, Shoji Noguchi, Masanori Katsuyama, Masamitsu Fujimoto, Yoshiko Kosugi, Ushio Kurokawa, Eiichi Nakakita, Kenji Tsuruta, Hiroki Iwata, and Yasuhisa Kuzuha. Acknowledgement is extended to Nobuo Toride and Masaru Sakai for their kind teaching of HYDRUS and Forestry and Forest Products Research Institute for the use of observational data in the Tatsunokuchiyama Experimental Watershed. This paper was also supported by the Coca-Cola Foundation to a study on "the impact of forest on water cycle and climate change".

Appendix 1. Applicability of storage function model to hillslope-scale observational results

We examine whether the application of SFE to runoff responses in CAPs at a watershed scale can be applied at a hillslope scale. This assessment is made because scale issues derived from spatial differences from hillslopes to watersheds have been widely discussed in hydrology (Blöschl and Sivapalan, 1995; Sivapalan, 2003; McGuire et al., 2005; Clark et al., 2009; Asano et al., 2009; Sidle et al., 2017). Hence, we reanalyze a hydrometric observation on a steep planar hillslope with a thin soil layer.

A1.1. Site description of study hillslope

For this examination, storm records in July 1987 on a steep planar hillslope without a riparian corridor in the Tatsunokuchi-yama Experimental Watershed, Okayama, Japan were assessed (Fig. A1). These observations were conducted by the Forestry and Forest Products Research Institute and the data analysis and site description were reported by Tani (1997). A long-term hydrological study in a small watershed, Minamitani (MN: 22.6 ha) in Tatsunokuchi-yama, has continued since 1937, and runoff responses to storms have been assessed by several studies (Tani and Abe, 1987; Tani et al., 2012; Hosoda and Tani, 2016). Our study hillslope (SL) located inside of the MN watershed is underlain by quartz porphyry although about 96% of the watershed is underlain by Paleozoic rock formations.

The topography of the SL is steep (34.6°) and short (42.7 m), and the soil layer is thin compared with most slopes in MN. Runoff discharge from a trench at the toe of the slope was monitored using a 6 m long brick wall tightly fixed to the exposed bedrock along the stream channel. The contributing area of SL was estimated at 500 m^2 ; average width was 11.7 m, and slope length was 42.7 m. This width is larger than the bottom width (6 m), suggesting that water flow converges from the wider upslope area despite its planar surface topography. Soil textures are clay loam and sandy loam produced from the bedrock, and the saturated hydraulic conductivity was estimated as 1.7 to $6.3 \times 10^{-3} \text{ cm s}^{-1}$. Observations of the soil profile at the trench showed that the mineral soil contained many macropores which preferentially produced much runoff discharge during storms. An old landslide scar existed halfway up the slope with bedrock exposed at the headwall of the landslide. Soil depth varied along the slope with an average depth of about 50 cm.

In addition to measuring runoff discharge, pressure head was monitored at 10, 30, and 50 cm depths at T4, 11.0 m upslope from the trench. These observed values were used to examine the applicability of the Richards equation to the pressure head propagation. The observations in SL were conducted between January 1986 and November 1987.

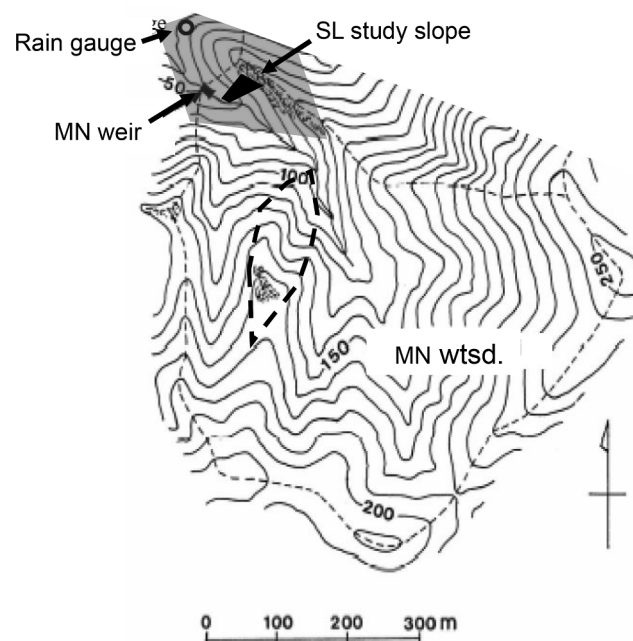


Fig. A1. Location map of Minamitani catchment (MN) and study hillslope (SL) in the Tatsunokuchi-yama Experimental Watershed. Hatched area is underlain by quartz porphyry but other is by Paleozoic rock formations. The area surrounded by a thick-dashed line indicates study hillslope observed by Hosoda and Tani (2016).

A1.2. Model applicability

The basic characteristics of storm runoff responses for SL were similar to those for the entire MN watershed, despite different geology, topography, and spatial scale (Tani and Abe, 1987; Tani, 1997). Fig. A2 shows relationships of total storm rainfall and runoff at SL and MN. The relationships between the cumulative rainfall and storm runoff for our target storm event in July 1987 (the total rainfall = 137 mm) and total runoff from MN and SL (48 mm and 69 mm, respectively) are plotted in panels (Fig. A2a) and (Fig. A2b). In addition, the relationship for an event in September 1976, in which the total rainfall and storm runoff were 375 and 248 mm, respectively, one of the largest storms in the 80-year observation periods of MN, is also plotted in Fig. A2(a).

In both MN and SL, when rainfall was small, total storm runoff was very low because most of the rainwater was stored in the soil, and this storage effect depends on antecedent moisture conditions, as indicated by the initial runoff rates of MN before the event. In both MN and SL, storm runoff occur until a threshold of rainfall was reached, although this value depends on the antecedent moisture conditions. The rate of increase in storm

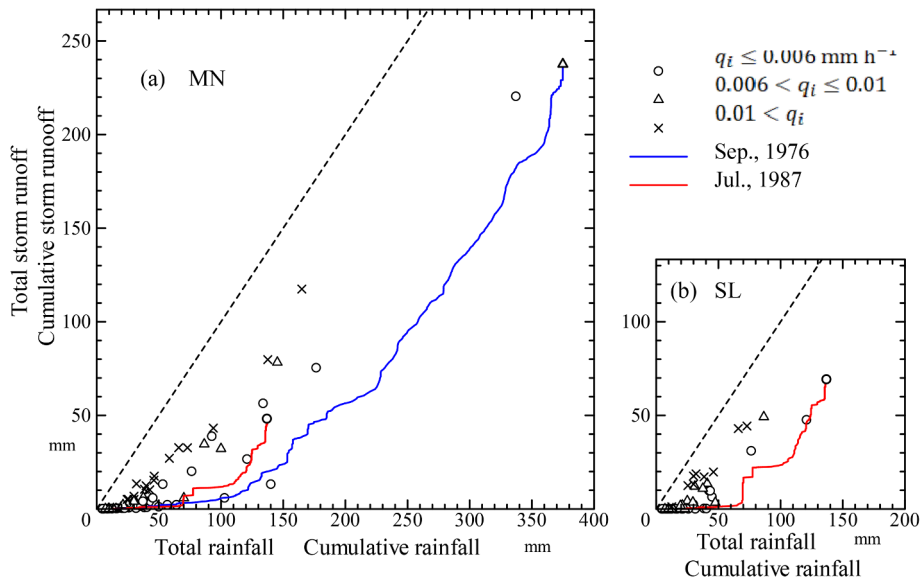


Fig. A2. Total storm rainfall and runoff relationships for MN (a) and SL (b). q_i : the initial runoff rate of MN. The blue and red lines indicate the relationships between cumulative rainfall and storm runoff in the storm events in September 1976 and in July 1987, respectively.

runoff was similar to that of rainfall during large storms as shown in the cumulative relationship for the storm of 1976 (Fig. A2a). Although this tendency occurred in both MN and SL (Fig. A2b), the steeper increase in storm runoff for SL compared to MN may be caused by a more rapid extension of the stormflow contributing area likely due to the short and steep topography and thin soil layer in SL compared to the averaged slope properties of MN (Tani, 1997). Hence, when cumulative rainfall is large enough, the concept of ‘saturated rainfall’ in SFM is applicable not only to the small watershed scale (MN) but also to the planar hillslope (SL).

During the 1976 storm, the threshold for runoff increase in MN occurred around 2:00 on September 10 (Fig. A3), and the cumulative rainfall and storm runoff volumes up to this threshold were 67 and 4 mm, respectively. The CAP was achieved around 14:00 on September 11, and the cumulative rainfall and storm runoff volumes up to this time were 186 and 54 mm, respectively. Therefore, three stages in the runoff generation mechanism can be distinguished as follows; (1) initially, rainwater falling onto most of the entire watershed was absorbed in the dry soil in the first dry stage; (2) then, the area contributing to stormflow generation was extended over the entire catchment; and (3) finally the contributing area was fixed to the entire watershed because total storm runoff (186 mm) in this period was almost equal to total rainfall (189 mm). Interestingly, a similar and constant value (5.4 mm h^{-1}) for both rainfall intensity and runoff rate occurred from 10:00 to 14:00 on September 12, suggesting a steady state response to constant rainfall intensity was achieved in this period for the entire MN watershed. To examine the applicability of SFE to the runoff responses, this equation set was applied to the storm event by optimizing the parameter values for the hydrograph in the third stage (CAP) using the method of least squares; optimized values of p and k are 0.3 and $40 \text{ mm}^{0.7} \text{ h}^{0.3}$, respectively (Fig. A3). The comparison between observed and calculated hydrographs clearly demonstrates a distinction in the characteristics of the three stages as well as good agreement between the result calculated by SFE with the observed hydrograph in the third stage.

Runoff responses in MN and SL during a storm in July 1987 were compared with those calculated by SFE, where the parameters for MN were the same as those in the 1976 storm (Fig. A3). CAP was not fully achieved for MN because the calculated hydrograph was higher than the observed hydrograph, but the second transient stage continued until the end of the event. For SL, however, the hydrograph calculated using the optimized k value ($27 \text{ mm}^{0.7} \text{ h}^{0.3}$) (obtained by the method of least squares) for the same p value (0.3) agreed with the observed hydrograph in the final stage of this event after 2:00 on July 19. Hence, the CAP may be roughly achieved although the total runoff (47 mm) in this duration was somewhat smaller than the total rainfall (60 mm) and a small portion of rainfall was not contributing to storm runoff.

We can therefore conclude that the applicability of SFE is valid for storm runoff responses at a hillslope scale as well as at a small watershed scale, although the cumulative rainfall necessary to achieve CAP was smaller (Fig. A2) and the hydrograph is steeper (Fig. A4) for SL than MN.

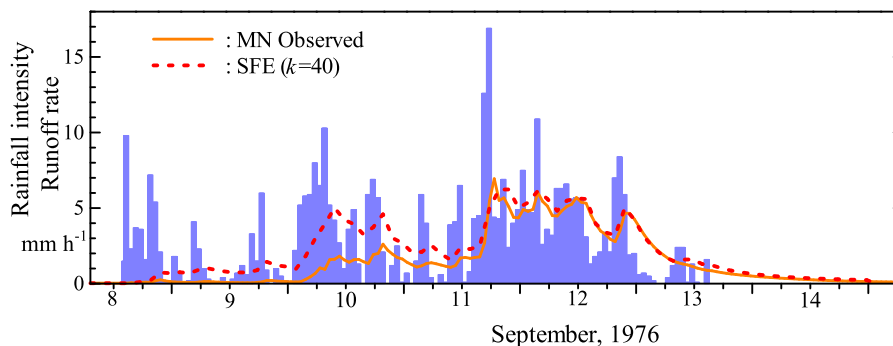


Fig. A3. Comparison between observed hydrograph with that calculated by SFE for one of the largest storm events in September 1976 for MN.

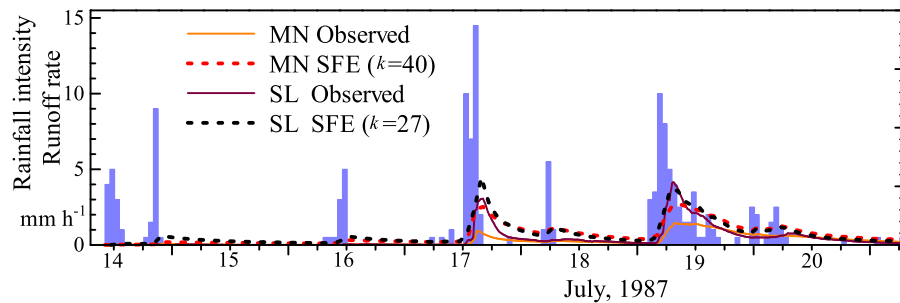


Fig. A4. Comparison between observed hydrograph with that calculated by SFE for a storm event in July 1987 for MN and SL.

References

- Ali, G., Oswald, C.J., Spence, C., Cammeraat, E.L.H., McGuire, K.J., Meixner, T., Reaney, S.M., 2013. Towards a unified threshold-based hydrological theory: necessary components and recurring challenges. *Hydrol. Process.* 27, 313–318. <https://doi.org/10.1002/hyp.9560>.
- Anderson, S.P., Dietrich, W.E., Montgomery, D.R., Torres, R., Conrad, M.E., Loague, K., 1997. Subsurface flow paths in a steep, unchanneled catchment. *Water Resour. Res.* 33, 2637–2653.
- Arnaud, P., Lavabre, J., Fouchier, C., Diss, S., Javelle, P., 2011. Sensitivity of hydrological models to uncertainty in rainfall input. *Hydrol. Sci. J.* 56, 397–410. <https://doi.org/10.1080/02626667.2011.563742>.
- Asano, Y., Uchida, T., Mimasu, Y., Ohte, N., 2009. Spatial patterns of stream solute concentrations in a steep mountainous catchment with a homogeneous landscape. *Water Resour. Res.* 45. <https://doi.org/10.1029/2008WR007466>.
- Bergström, S., Forsman, A., 1973. Development of a conceptual deterministic rainfall-runoff model. *Nordic Hydrol.* 4, 147–170.
- Beven, K., 1984. Infiltration into a class of vertically non-uniform soils. *Hydrol. Sci. J.* 29, 425–434.
- Beven, K., 2012. *Rainfall-Runoff Modelling: The Primer, Second Edition*. Wiley & Sons, Chichester 488 p.
- Blöschl, G., Sivapalan, M., 1995. Scale issues in hydrological modelling: a review. *Hydrol. Process.* 9, 251–290.
- Boggard, T.A., Greco, R., 2015. Landslide hydrology: from hydrology to pore pressure. *Wiley Interdisc. Rev. Water* 3 (3). <https://doi.org/10.1002/wat2.1126>.
- Buttle, J.M., McDonald, D.J., 2002. Coupled vertical and lateral preferential flow on a forested slope. *Water Resour. Res.* 38, 2002. <https://doi.org/10.1029/2001WR000773>.
- Chiffard, P., Blume, T., Maerker, K., Hopp, L., van Meerveld, I., Graef, T., Gronz, O., Hartmann, A., Kohl, B., Martini, E., Reinhardt-Imjela, C., Reiss, M., Rinderer, M., Achleitner, S., 2019. How can we model subsurface stormflow at the catchment scale if we cannot measure it? *Hydrol. Process.* doi: 10.1002/hyp.13407.
- Clark, M.P., Rupp, D.E., Woods, R.A., Tromp-van Meerveld, H.J., Peters, N.E., Freer, J.E., 2009. Consistency between hydrological models and field observations: linking processes at the hillslope scale to hydrological responses at the watershed scale. *Hydrol. Process.* 23, 311–319. <https://doi.org/10.1002/hyp.7154>.
- Dusek, J., Vogel, T., 2016. Hillslope-storage and rainfall-amount thresholds as controls of preferential stormflow. *J. Hydrol.* 534, 590–605. <https://doi.org/10.1016/j.jhydrol.2016.01.047>.
- Dusek, J., Vogel, T., Dohnal, M., Gerke, H.H., 2012. Combining dual-continuum approach with diffusion wave model to include a preferential flow component in hillslope scale modeling of shallow subsurface runoff. *Adv. Water Resour.* 44, 113–125. <https://doi.org/10.1016/j.advwatres.2012.05.006>.
- Ebel, B.A., Loague, K., Montgomery, D.R., Dietrich, W.E., 2007. Physics-based continuous simulation of long-term near-surface hydrologic response for the Coos Bay experimental catchment. *Water Resour. Res.* 44, 2007. <https://doi.org/10.1029/2007WR006442>.
- Ebel, B.A., Loague, K., 2008. Rapid simulated hydrologic response within the variably saturated near surface. *Hydrol. Process.* 22, 464–471. <https://doi.org/10.1002/hyp.6926>.
- Fatchi, S., Vivoni, E.R., Ogdin, F.L., Ivanov, V.Y., Mirus, B., Gochis, D., Downer, C.W., Camporese, M., Davison, J.H., Ebel, B., Jones, N., Kim, J., Mascarom, G., Niswonger, R., Restrepo, P., Rigon, R., Shen, C., Sulis, M., Tarboton, D., 2016. An overview of current applications, challenges, and future trends in distributed process-based models in hydrology. *J. Hydrol.* 537, 45–60. <https://doi.org/10.1016/j.jhydrol.2016.03.026>.
- Fukushima, Y., Suzuki, M., 1988. A model for river flow forecasting for a small mountain catchment. *Hydrol. Process.* 2, 167–185.
- Gerke, H.H., van Genuchten, M.T., 1993. A dual-porosity model for simulating the preferential movement of water and solutes in structured porous media. *Water Resour. Res.* 29, 305–319.
- Ghstem, M., Sidle, R.C., Stokes, A., 2011. The influence of plant root systems on subsurface flow: implications for slope stability. *Bioscience* 61, 869–879. <https://doi.org/10.1525/bio.2011.61.11.6>.
- Gomi, T., Asano, Y., Uchida, T., Onda, Y., Sidle, R.C., Miyata, S., Kosugi, K., Mizugaki, S., Fukuyama, T., 2010. Evaluation of storm runoff pathways in steep nested catchments draining a Japanese cypress forest in central Japan: a hydrometric, geochemical, and isotopic approaches. *Hydrol. Process.* 24, 550–566. <https://doi.org/10.1002/hyp.7550>.
- Gopalan, S.P., Kawamura, A., Takasaki, T., Amaguchi, H., Azhikodan, G., 2018. An effective storage function model for an urban watershed in terms of hydrograph reproducibility and Akaike information criterion. *J. Hydrol.* 563, 657–668. <https://doi.org/10.1016/j.jhydrol.2018.06.035>.
- Graham, C., McDonnell, J.J., 2010. Hillslope threshold response to rainfall: (2) development and use of a macroscale model. *J. Hydrol.* 393, 77–93. <https://doi.org/10.1016/j.jhydrol.2010.03.008>.
- Guo, L., Chen, J., Lin, H., 2014. Subsurface lateral preferential flow network revealed by time-lapse ground-penetrating radar in a hillslope. *Water Resour. Res.* 50, 9127–9147. <https://doi.org/10.1002/2013WR014603>.
- Heimsath, A.M., Dietrich, W.E., Nishiizumi, K., Finkel, R.C., 1999. Cosmogenic nuclides, topography, and the spatial variation of soil depth. *Geomorphology* 27, 151–172.
- Hewlett, J.D., Hibbert, A.R., 1967. Factors affecting the response of small watersheds to precipitation in humid areas. In: *Proceedings of 1st International Symposium on Forest Hydrology*, pp. 275–290.
- Hosoda, I., Tani, M., 2016. Influence of moisture fluctuations in thick, weathered bedrock layers on rainfall-runoff response in a small, forested catchment underlain by Paleozoic sedimentary rocks in Japan. *Trans. Jpn. Geomorph. Union* 37, 465–492 (in Japanese with English abstract).
- Istanbulluoglu, E., Bras, R.L., 2005. Vegetation-modulated landscape evolution: effects of vegetation on landscape processes, drainage density, and topography. *J. Geophys. Res.* 110. <https://doi.org/10.1029/2004JF000249>.
- Iwasaki, K., Katsuyama, M., Tani, M., 2015. Contributions of bedrock groundwater to the upscaling of storm-runoff generation processes in weathered granitic headwater catchments. *Hydrol. Process.* 29, 1535–1548. <https://doi.org/10.1002/hyp.10279>.
- Katsuyama, M., Fukushima, K., Tokuchi, N., 2008. Comparison of rainfall-runoff characteristics in forested catchments underlain by granitic and sedimentary rock with various forest age. *Hydrol. Res. Lett.* 2, 14–17.
- Kimura, T., 1961. The flood runoff analysis method by the storage function model. *Civil Eng. Mater.* (published by The Public Works Research Institute, Ministry of Construction, Japan) 3 (12), 36–43 (in Japanese).
- Kimura, T., 1975. *The Storage Function Model*. Publishing Company Kawanabe, Tokyo (in Japanese).
- Kitahara, H., 1993. Characteristics of pipe flow in forested slopes, exchange processes of the land surface for a range of space and time scales. *IAHS Publ.* 212, 235–242.
- Kosugi, K., 1994. Three-parameter lognormal distribution model for soil water retention. *Water Resour. Res.* 30, 891–901.
- Kosugi, K., 1996. Lognormal distribution model for unsaturated soil hydraulic properties. *Water Resour. Res.* 32, 2697–2703.
- Kosugi, K., 1997a. A new model to analyze water retention characteristics of forest soils based on soil pore radius distribution. *J. For. Res.* 2, 1–8.
- Kosugi, K., 1997b. New diagrams to evaluate soil pore radius distribution and saturated hydraulic conductivity of forest soil. *J. For. Res.* 2, 95–101.
- Kosugi, K., Fujimoto, M., Katsura, S., Kato, H., Sando, Y., Mizuyama, T., 2011. Localized bedrock aquifer distribution explains discharge from a headwater catchment. *Water Resour. Res.* 47. <https://doi.org/10.1029/2010WR009884>.
- Liang, W., Kosugi, K., Mizuyama, T., 2009. A three-dimensional model of the effect of stemflow on soil water dynamics around a tree on a hillslope. *J. Hydrol.* 366, 62–75. <https://doi.org/10.1016/j.jhydrol.2008.12.009>.
- Liang, W., Kosugi, K., Mizuyama, T., 2011. Soil water dynamics around a tree on a hillslope with or without rainwater supplied by stemflow. *Water Resour. Res.* 47. <https://doi.org/10.1029/2010WR009856>.
- Madsen, H., 2000. Automatic calibration of a conceptual rainfall-runoff model using multiple objectives. *J. Hydrol.* 235, 276–288.
- Mashimo, Y., 1960. Studies on the physical properties of forest soil and their relation to the growth of sugi (*Cryptomeria japonica*) and hinoki (*Chamaecyparis obtusa*). *For. Soils Jpn.* 11, 1–182 (in Japanese with English summary).
- Matsushi, Y., Matsuzaki, H., 2010. Denudation rates and threshold slope in a granitic watershed, central Japan. *Nucl. Instr. Meth. Phys. B* 268, 1201–1204. <https://doi.org/10.1016/j.nimb.2009.10.133>.
- Matsushi, Y., Toyama, M., Matsuzaki, H., Chigira, M., 2016. Simulation of soil production and transport for prediction of location and magnitude of shallow landslides. *Trans. Japan. Geomorph. Union* 37, 427–453 (in Japanese with English abstract).
- McDonnell, J.J., 1990. A rationale for old water discharge through macropores in a steep, humid catchment. *Water Resour. Res.* 26, 2821–2832.
- McDonnell, J.J., Sivapalan, M., Vaché, K., Dunn, S., Grant, G., Haggerty, R., Hinz, C., Hooper, R., Kirchner, J., Roderick, M.L., Selker, J., Weiler, M., 2007. Moving beyond heterogeneity and process complexity: a new vision for watershed hydrology. *Water Resour. Res.* 43. <https://doi.org/10.1029/2006WR005467>.
- McGuire, K.J., McDonnell, J.J., Weiler, M., Kendall, C., McGlynn, B.L., Welker, J.M.,

- Seibert, J., 2005. The role of topography on catchment-scale water residence time. *Water Resour. Res.* 41. <https://doi.org/10.1029/2004WR003657>.
- Milledge, D.G., Bellugi, D., McKean, J.A., Densmore, A.L., Dietrich, W.E., 2014. A multidimensional stability model for predicting shallow landslide size and shape across landscapes. *J. Geophys. Res. Earth Surf.* 119, 2481–2504. <https://doi.org/10.1002/2014JF003135>.
- Miller, E.E., Miller, R.D., 1956. Physical theory for capillary flow phenomena. *J. Appl. Phys.* 27, 324–332.
- Mirus, B.B., Loague, K., 2013. How runoff begins (and ends): Characterizing hydrologic response at the catchment scale. *Water Resour. Res.* 49, 2987–3006. <https://doi.org/10.1002/wrcr.20218>.
- Miyata, S., Kosugi, K., Gomi, T., Mizuyama, T., 2009. Effects of forest floor coverage on overland flow and soil erosion on hillslopes in Japanese cypress plantation forests. *Water Resour. Res.* 45. <https://doi.org/10.1029/2008WR007270>.
- Montgomery, D.R., Dietrich, W.E., 2002. Runoff generation in a steep, soil-mantled landscape. *Water Resour. Res.* 38. <https://doi.org/10.1029/2001WR000822>.
- Montgomery, D.R., Dietrich, W.E., Torres, R., Anderson, S.P., Heffner, J.T., Loague, K., 1997. Hydrologic response of a steep, unchanneled valley to natural and applied rainfall. *Water Resour. Res.* 33, 91–109.
- Montgomery, D.R., Schmidt, K.M., Dietrich, W.E., McKean, J., 2009. Instrumental record of debris flow initiation during natural rainfall: Implications for modeling slope stability. *J. Geophys. Res.* 114. <https://doi.org/10.1029/2008JF001078>.
- Mualem, Y., 1976. A catalogue of the Hydraulic Properties of Unsaturated Soils. Technion-Israel Inst. of Technol., Haifa.
- Murakami, S., 2006. A proposal for a new forest canopy interception mechanism: Splash droplet evaporation. *J. Hydrol.* 319, 72–82.
- Nanko, K., Onda, Y., Ito, A., Ito, S., Mizugaki, S., Moriwaki, H., 2010. Variability of surface runoff generation and infiltration rate under a tree canopy: indoor rainfall experiment using Japanese cypress (*Chamaecyparis obtusa*). *Hydrol. Process.* 24, 567–575. <https://doi.org/10.1002/hyp.7551>.
- Nash, J.E., 1960. A unit hydrograph study with particular reference to British catchments. *Proc. Inst. Civil Eng.* 17, 249–282.
- Noguchi, S., Abdul, Rahim N., Zulkifli, Y., Tani, M., Sammori, T., 1997. Rainfall-runoff responses and roles of soil moisture variations to the response in tropical rain forest, Bukit Tarek, Peninsular Malaysia. *J. For. Res.* 2, 125–132.
- Noguchi, S., Tsuboyama, Y., Sidle, R.C., Hosoda, I., 1999. Morphological characteristics of macropores and the distribution of preferential flow pathways in a forested slope segment. *Soil Sci. Soc. Am. J.* 63, 1413–1423. <https://doi.org/10.2136/sssaj1999.6351413x>.
- Ohta, T., Fukushima, Y., Suzuki, M., 1983. Research on runoff from hillsides by one-dimensional transient saturated-unsaturated flow. *J. Jpn. For. Soc.* 65, 125–134 (in Japanese with English abstract).
- Onda, Y., Komatsu, Y., Tsujimura, M., Fujihara, J., 2001. The role of subsurface runoff through bedrock on storm flow generation. *Hydrol. Process.* 15, 1693–1706. <https://doi.org/10.1002/hyp.234>.
- Park, J., Kang, I.S., Singh, V.P., 1999. Comparison of simple runoff models used in Korea for small watersheds. *Hydrol. Process.* 13, 1527–1540.
- Pearce, A.J., Stewart, M.K., Sklash, M.G., 1986. Storm runoff generation in humid headwater catchments: 1. Where does the water come from? *Water Resour. Res.* 22, 1263–1272.
- Project for the Enhancement of Capabilities in Flood Control and Sabo Engineering of the DPWH, 2002. Technical Standards and Guidelines for Planning and Design, Vol. 1 Flood Control. Department of Public Works and Highways, Japan International Cooperation Agency, Tokyo.
- Retter, M., Kienzler, P., Germann, P.F., 2006. Vectors of subsurface stormflow in a layered hillslope during runoff initiation. *Hydrol. Earth Syst. Sci.* 10, 309–320.
- Roering, J.J., Almond, P., Tonkin, P., McKean, J., 2002. Soil transport driven by biological processes over millennial time scales. *Geology* 30, 1115–1118.
- Shimokawa, E., 1984. A natural recovery process of vegetation on landslide scars and landslide periodicity in forested drainage basins. In: *Proc. Symposium Effects of Forest Land Use on Erosion and Slope Stability*. University of Hawaii, Honolulu, pp. 99–107.
- Sidle, R.C., Bogaard, T.A., 2016. Dynamic earth system and ecological controls of rainfall-initiated landslides. *Earth-Sci. Rev.* 159, 275–291. <https://doi.org/10.1016/j.earscirev.2016.05.013>.
- Sidle, R.C., Gomi, T., Loaiza Usuga, J.C., Jarihani, B., 2017. Hydrogeomorphic processes and scaling issues in the continuum from soil pedons to catchments. *Earth-Sci. Rev.* 175, 75–96. <https://doi.org/10.1016/j.earscirev.2017.10.010>.
- Sidle, R.C., Kitahara, H., Terajima, T., Nakai, Y., 1995. Experimental studies on the effects of pipeflow on throughflow partitioning. *J. Hydrol.* 165, 207–219.
- Sidle, R.C., Noguchi, S., Tsuboyama, Y., Laursen, K., 2001. A conceptual model of preferential flow systems in forested hillslopes: evidence of self-organization. *Hydrol. Process.* 15, 1673–1674.
- Sidle, R.C., Tsuboyama, Y., Noguchi, S., Hosoda, I., Fujiwada, M., Shimizu, T., 2000. Stormflow generation in steep forested headwaters: a linked hydrogeomorphic paradigm. *Hydrol. Process.* 14, 369–385.
- Sidle, R.C., Ziegler, A.D., Negishi, J., Abdul, Rahim N., Siew, R., Turkelboom, F., 2006. Erosion processes in steep terrain: truths, myths, and uncertainties related to forest management in Southeast Asia. *For. Ecol. Manage.* 224, 199–225. <https://doi.org/10.1016/j.foreco.2005.12.019>.
- Šimůnek, J., Šejna, M., Saito, H., Sakai, S., van Genuchten, M.T., 2013. The Hydrus-1D software package for simulating the movement of water, heat, and multiple solutes in variably saturated media, Version 4.17, HYDRUS Software Series 3. Department of Environmental Sciences, University of California Riverside, Riverside.
- Sivapalan, M., 2003. Process complexity at hillslope scale, process simplicity at the watershed scale: is there a connection? *Hydrol. Process.* 17, 1037–1041.
- Smith, R.E., 1983. Approximate soil water movement by kinematic characteristics. *Soil Sci. Soc. Am. J.* 47 (3–8), 1983.
- Sudicky, E.A., Jones, J.P., Park, Y.J., Brookfield, A.E., Colautti, D., 2008. Simulating complex flow and transport dynamics in an integrated surface-subsurface modeling framework. *Geosci. J.* 12, 107–122. <https://doi.org/10.1007/s12303-008-0013-x>.
- Sueishi, T., 1955. On the run-off analysis by the method of characteristics – hydraulic studies on the run-off phenomena of rain water, 2nd report. *Trans. JSCE* 29, 74–87 (in Japanese with English abstract).
- Sugawara, M., 1961. On the analysis of runoff structure about several Japanese River. *Jpn. J. Geophys.* 4 (2), 1–76.
- Sugawara, M., 1995. Tank model. In: Singh, V.J. (Ed.), *Computer Models in Watershed Hydrology*. Water Resources Publications, Highland Ranch, pp. 165–214.
- Sugiyama, H., Kadoya, M., Nagai, A., Lansey, K., 1997. Evaluation of the storage function model parameter characteristics. *J. Hydrol.* 191, 332–348.
- Supraba, I., Yamada, T., 2015. Potential water storage capacity of mountainous catchments based on catchment characteristics. *J. JSCE, B1 (Hydraul. Eng.)* 71 (4), 1151–1156.
- Tani, M., 1982. The properties of a water-table rise produced by a one-dimensional, vertical, unsaturated flow. *J. Jap. For. Soc.* 64, 409–418 (in Japanese with English abstract).
- Tani, M., 1985a. Analysis of one-dimensional, vertical, unsaturated flow in consideration of runoff properties of a mountainous watershed. *J. Jap. For. Soc.* 67, 449–460 (in Japanese with English abstract).
- Tani, M., 1985b. The effects of soil physical properties on the groundwater-table rise. In: *International Symposium on Erosion, Debris Flow and Disaster Prevention*, Tsukuba, pp. 361–365.
- Tani, M., 1996. An approach to annual water balance for small mountainous catchments with wide spatial distributions of rainfall and snow water equivalent. *J. Hydrol.* 183, 205–225.
- Tani, M., 1997. Runoff generation processes estimated from hydrological observations on a steep forested hillslope with a thin soil layer. *J. Hydrol.* 200, 84–109.
- Tani, M., 2008. Analysis of runoff storage relationships to evaluate the runoff-buffering potential of a sloping permeable domain. *J. Hydrol.* 360, 132–146. <https://doi.org/10.1016/j.jhydrol.2008.07.023>.
- Tani, M., 2013. A paradigm shift in stormflow predictions for active tectonic regions with large-magnitude storms: generalisation of catchment observations by hydraulic sensitivity analysis and insight into soil-layer evolution. *Hydrol. Earth Syst. Sci.* 17, 4453–4470. <https://doi.org/10.5194/hess-17-4453-2013>.
- Tani, M., Abe, T., 1987. Analysis of stormflow and its source area expansion through a simple kinematic wave equation. *For. Hydrol. Watershed Manag. IAHS Publ.* 167, 609–615.
- Tani, M., Fujimoto, M., Katsuyama, M., Kojima, N., Hosoda, I., Kosugi, K., Kosugi, Y., Nakamura, S., 2012. Predicting the dependencies of rainfall-runoff responses on human forest disturbances with soil loss based on the runoff mechanisms in granitic and sedimentary-rock mountains. *Hydrol. Process.* 26, 809–826. <https://doi.org/10.1002/hyp.8295>.
- Torres, R., Dietrich, W.E., Montgomery, D.R., Anderson, S.P., Loague, K., 1998. Unsaturated zone processes and the hydrologic response of a steep, unchanneled catchment. *Water Resour. Res.* 34, 1865–1879.
- Troch, P.A., Carrillo, G.A., Heidbüchel, I., Rajagopal, S., Switanek, M., Volkman, T.H.M., Yaeger, M., 2009. Dealing with landscape heterogeneity in watershed hydrology: a review of recent progress toward new hydrological theory. *Geogr. Compass* 3, 375–392. <https://doi.org/10.1111/j.1749-8198.2008.00186.x>.
- Tsuboyama, Y., Sidle, R.C., Noguchi, S., Hosoda, I., 1994. Flow and solute transport through the soil matrix and macropores of a hillslope segment. *Water Resour. Res.* 30, 879–890.
- Tsukamoto, Y., Minematsu, H., 1987. Evaluation of the effect of deforestation on slope stability and its application to watershed management. *Proceedings of the Vancouver Symposium IAHS Publ.* 167, 181–189.
- Tsutsumi, D., Sidle, R.C., Kosugi, K., 2005. Development of a simple lateral preferential flow model with steady state application in hillslope soils. *Water Resour. Res.* 41. <https://doi.org/10.1029/2004WR003877>.
- Uchida, T., Asano, Y., Ohte, N., Mizuyama, T., 2003. Analysis of flowpath dynamics in a steep unchanneled hollow in the Tanakami Mountains of Japan. *Hydrol. Process.* 17, 417–430. <https://doi.org/10.1002/hyp.1133>.
- Uchida, T., Tromp-van Meerveld, I., McDonnell, J.J., 2005. The role of lateral pipe flow in hillslope runoff response: an intercomparison of non-linear hillslope response. *J. Hydrol.* 311, 117–133. <https://doi.org/10.1016/j.jhydrol.2005.01.012>.
- VanderKwaak, J.E., Loague, K., 2001. Hydrologic-response simulations for the R-5 catchment with a comprehensive physics-based model. *Water Resour. Res.* 37, 999–1013.
- van Genuchten, M.T., 1980. A closed-form equation for predicting the hydraulic conductivity of unsaturated soils. *Soil Sci. Soc. Am. J.* 44, 892–898.
- Verma, R.D., Brutsaert, W., 1970. Unconfined aquifer seepage by capillary flow theory. *J. Hydraul. Div. ASCE* 96, 1331–1344.
- Vogel, T., Breznina, J., Dohal, M., Dusek, J., 2010. Physical and numerical coupling in dual-continuum modeling of preferential flow. *Vadose Zone J.* 9, 260–267. <https://doi.org/10.2136/vzj2009.0091>.
- Watakabe, T., Matshushi, Y., 2019. Lithological controls on hydrological processes that trigger shallow landslides: observations from granite and hornfels hillslopes in Hiroshima, Japan. *Catena* 180, 55–68. <https://doi.org/10.1016/j.catena.2019.04.010>.
- Wu, S.J., Ho, L.F., Yang, J.C., 2011. Application of modified nonlinear storage function on runoff estimation. *J. Hydro. Environ. Res.* 5, 37–47. <https://doi.org/10.1016/j.jher.2010.09.003>.